Geochemistry Geophysics Geosystems G3
AN ELECTRONIC JOURNAL OF THE EARTH SCIENCES
Published by AGU and the Geochemical Society

Article
Volume 9, Number 6
28 June 2008
Q06012, doi:10.1029/2007GC001799
ISSN: 1525-2027

Internal structure of a contourite drift generated by the Antarctic Circumpolar Current

Dorit Koenitz
Bullard Laboratories, Department of Earth Sciences, University of Cambridge, Madingley Rise, Madingley Road, Cambridge CB3 0EZ, UK

Now at PGS Geophysical AS, Standveien 4, P.O. Box 290, 1326 Lysaker, Norway

Nicky White and I. Nick McCave
Bullard Laboratories, Department of Earth Sciences, University of Cambridge, Madingley Rise, Madingley Road, Cambridge CB3 0EZ, UK (nwhite@esc.cam.ac.uk)

Richard Hobbs
Bullard Laboratories, Department of Earth Sciences, University of Cambridge, Madingley Rise, Madingley Road, Cambridge CB3 0EZ, UK

Department of Earth Sciences, University of Durham, Durham DH1 3LE, UK

[1] We describe the internal structure and stratigraphy of a well-imaged contourite drift from the Southern Ocean. This drift, which we have named the South Falkland Slope Drift, lies on the northern flank of the Falkland Trough due south of the Falkland Islands. Drifts which occur directly in the path of the Antarctic Circumpolar Current (ACC), downstream of the Drake Passage gateway, are of considerable paleoceanographic significance since their detailed stratigraphic record will help to constrain the history of the ACC. We have reprocessed a grid of seismic reflection profiles generously provided by WesternGeco Ltd. in order to enhance imaging of the South Falkland Slope Drift and of drift deposits within the trough. The resultant high-quality images enable us to map the internal architecture of these drifts in unprecedented detail. By combining seismic stratigraphic mapping with measured sedimentation rates from nearby boreholes, we have inferred ages of the principal mappable horizons. With minor adjustments to sedimentation rates through time, we can show that these ages correspond to significant Southern Ocean events. We propose that the South Falkland Slope Drift initiated at 24.5–20.5 Ma, in accordance with some, but not all, published estimates of ACC establishment. A highly reflective horizon with an estimated age of 14.5 Ma corresponds to growth of the East Antarctic Ice Sheet, which led to a period of significant global cooling. A similarly bright reflective horizon with an estimated age of 9 Ma is thought to be related to a reorganization of bottom current flow which just predated establishment of grounded ice sheets on the Antarctic Peninsular shelf. Finally, a prominent early Pliocene unconformity at 4.5 Ma may be linked with the onset of major Northern Hemisphere glaciation or with Antarctic ice sheet expansion. We conclude that this well-imaged drift is an important, and largely continuous, stratigraphic record of ACC activity and suggest that it would be an excellent drilling target.

Components: 11819 words, 15 figures, 4 tables.

Keywords: contourite drift.

Index Terms: 0935 Exploration Geophysics: Seismic methods (3025, 7294); 3002 Marine Geology and Geophysics: Continental shelf and slope processes (4219); 4999 Paleoceanography: General or miscellaneous; 9310 Geographic Location: Antarctica (4207); 9605 Information Related to Geologic Time: Neogene.

Received 25 August 2007; **Revised** 8 February 2008; **Accepted** 5 March 2008; **Published** 28 June 2008.

Koenitz, D., N. White, I. N. McCave, and R. Hobbs (2008), Internal structure of a contourite drift generated by the Antarctic Circumpolar Current, *Geochem. Geophys. Geosyst.*, *9*, Q06012, doi:10.1029/2007GC001799.

1. Introduction

[2] The Antarctic Circumpolar Current (ACC) is the largest and strongest current system on Earth. It is responsible for the bulk of water mass exchange between the Pacific, Atlantic and Indian Oceans, transporting 100–140 Sv (1 Sv = 10^6 m^3 s^{-1}) from west to east around the Southern Ocean [*Grose et al.*, 1995; *Orsi et al.*, 1995; *Rintoul et al.*, 2001]. This inter-basinal exchange transports fresh water, heat, salt and nutrients globally [*Schmitz*, 1995; *Nowlin and Klinck*, 1986]. Thus anomalies formed in one basin can be carried to remote locations where they may influence climate [e.g., *White and Peterson*, 1996; *Rintoul et al.*, 2001]. Furthermore, deep circumpolar circulation is proposed as a key factor in the thermal isolation of East Antarctica and the triggering of major growth of ice sheets in the Oligocene [*Shackleton and Kennett*, 1975; *Zachos et al.*, 2001]. The detailed history of the ACC is of considerable interest, both on a Cenozoic timescale which includes cooling and glaciation of Antarctica, and on the timescale of Quaternary glacial cycles [*Gordon*, 2001].

[3] Although the ACC is essentially a westerly wind-driven flow over much of its path, it does extend to the sea bed where it controls sedimentation patterns, partly through strong flows along its fronts and partly through the more general eastward flow between fronts [*Barker*, 2001]. Consequently, the ACC should generate identifiable markers within the sedimentary record which can be used to constrain the nature and timing of tectonic, climatic, and oceanographic events [*Rack*, 1993; *Barker and Thomas*, 2004; *Pfuhl and McCave*, 2005; *Lyle et al.*, 2007]. These markers may manifest themselves as mappable discontinuities and changes in reflectivity patterns on seismic reflection data, or as changes in physical properties (e.g., bulk density, porosity, water content, grain size, consolidation) of sediments [*Rack*, 1993]. However, caution is necessary in seismic interpretation since the pattern of pre-ACC oceanic circulation is virtually unknown and sediment composition can also vary significantly as a function of biogenic activity [*Barker*, 2001].

[4] The Falkland Trough lies between the Falkland Plateau and Burdwood Bank, south of the Falkland Islands (Figure 1). The trough deepens from west to east, forming a pronounced bathymetric embayment presently occupied at its western end by the Sub-Antarctic Front (SAF). Present-day sedimentation is controlled by shallow-water components of the ACC, notably Antarctic Intermediate Water (AAIW) and Upper Circumpolar Deep Water (UCDW). AAIW is represented by a low-salinity layer that can be traced into the North Atlantic Ocean. Throughout the Southern Ocean, this layer is underlain by UCDW which is characterized by an oxygen minimum layer supplied by low-oxygen water from the Indian and Pacific basins [*Callahan*, 1972]. Emerging through a gap east of Burdwood Bank at 55°W which reaches 1700 m in depth, UCDW and AAIW flow westward into the Falkland Trough where they combine to form the Falkland Current which then follows the 1000 m isobath (Figure 1). At the western end of the trough, the shoaling sea bed acts as an obstacle, preventing further westward transport of water and deflecting flow northeastward at 60°W.

[5] The trough itself is a foreland basin generated by oblique shortening along the active boundary between the South American and Scotian plates [*Bry et al.*, 2004]. The geometry of this largely symmetrical and underfilled trough is clearly illustrated on Profiles 1, 3 and 5 in Figure 2a. South of the Falkland Islands, the active plate boundary along the southern margin of the trough consists of a set of thrust faults extending under Burdwood Bank, a large shallow plateau centered on 54°S, 59°W. The frontal, active fault is clearly visible at the southern edge of a prominent sea-bed moat on Profile 1 (Figure 2a). The structurally simpler northern margin of the trough is part of the Falkland Plateau which has been flexed down to the south, presumably by the encroaching crustal load represented by Burdwood Bank. This margin has

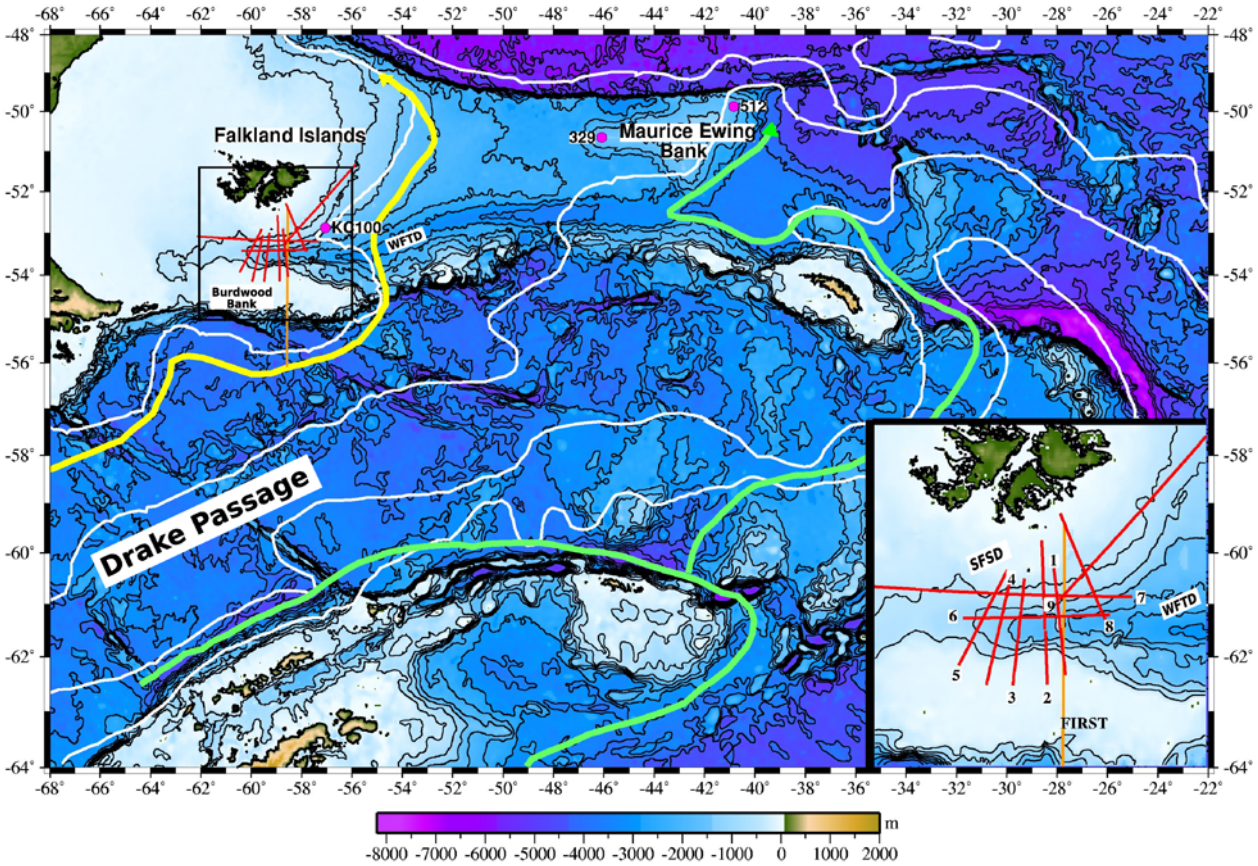

Figure 1. Bathymetric map of region encompassing Falkland Plateau which shows location of seismic reflection profiles used to image contourite drift (ETOPO5 [*Wessel and Smith*, 1998]). Inset shows Falkland Trough in more detail. Red numbered lines, WesternGeco lines used in this study (lines 1–5 were reprocessed at 2 ms); orange line, segment of Falkland Islands Regional Seismic Traverse (FIRST); thin white lines, major fronts of Antarctic Circumpolar Current; thick yellow and green lines, pathways of Antarctic Intermediate Circumpolar Water and Weddell Sea Deep Water, respectively; solid red circles, location of DSDP borehole and other cores used to constrain sedimentation rates.

been cut by closely spaced, north-dipping normal faults, some of which show demonstrable stratigraphic growth. A prominent unconformity is visible, separating overlying Neogene sediments from tilted and faulted Paleogene (?) and Mesozoic (?) strata. The most striking features on Profile 1 are the large contourite drift, which sits unconformably on top of the deflected northern margin, and the wedge of trough deposits (Figure 2a). *Howe et al.* [1997] and *Cunningham et al.* [2002] used 3.5 kHz records and low-fold seismic data to demonstrate the importance of Neogene-Recent contourite sedimentation on seismic reflection profiles further east. They showed that plastered drifts occur on the more exposed Falkland Plateau whereas confined and elongated drifts are more common within the relatively sheltered Falkland Trough. We are primarily concerned with the development of the large plastered drift which we refer to as the South Falkland Slope Drift (SFSD). *Cunningham et al.*'s [2002] West Falkland Trough Drift (WFTD) occurs east of the region we discuss here and it is confined to the trough itself. At the western end of this trough, our along-strike continuation of their WFTD probably consists of current-reworked turbiditic sediments, originally transported down channels from the west and north.

[6] Contourite drifts are linked to the action of semi-permanent bottom currents in deep water, usually resulting from thermohaline and/or wind-driven circulation in the oceans and their marginal seas. They are especially common along continental margins and at oceanic gateways [*Stow et al.*, 2002]. Both the SFSD and WFTD were deposited and reworked by vigorous bottom currents associated with flow of the ACC as it emerges from Drake Passage. These drift sediments record local

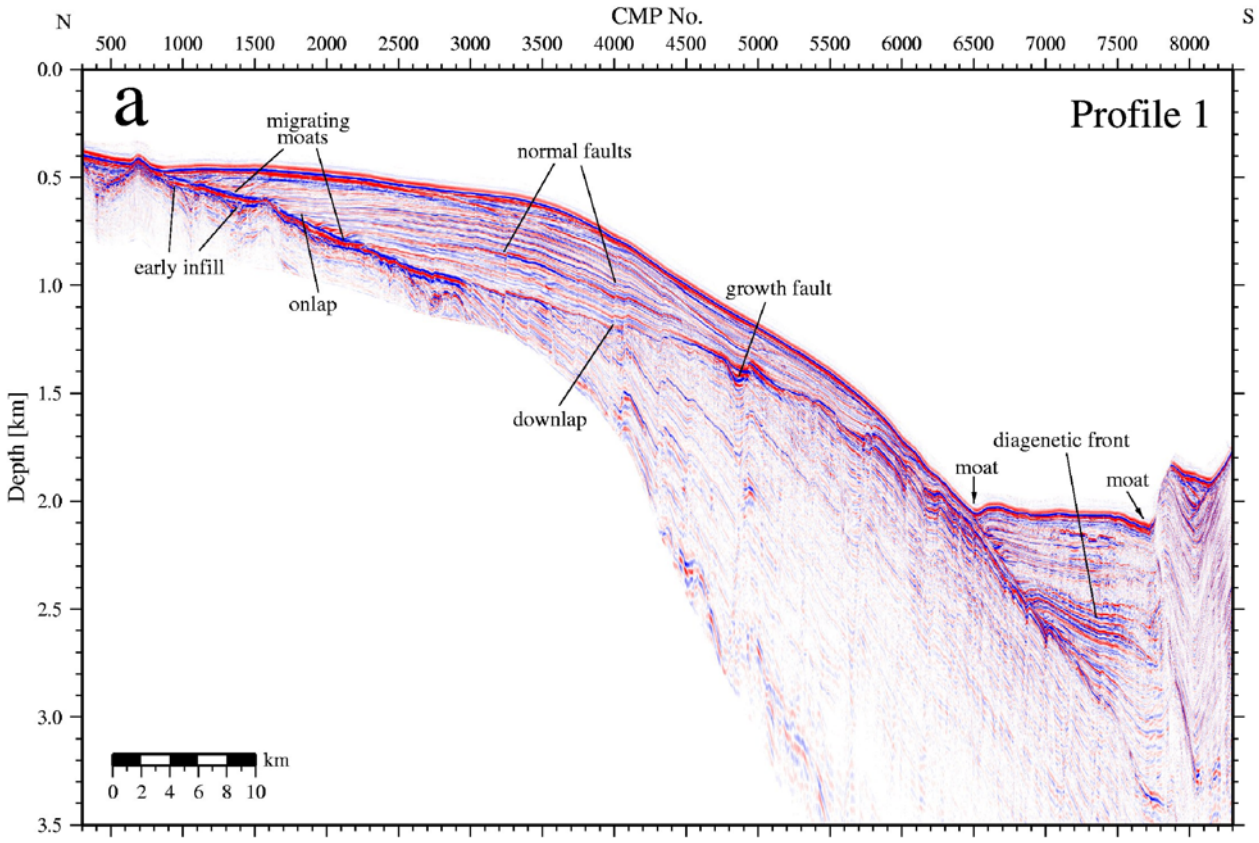

Figure 2. Three reprocessed and depth-converted (see Table 1) seismic reflection profiles which show general context and geometry of South Falkland Slope Drift (see Figure 1 for location). (a) Profile 1 provides clearest illustration of contourite drift whose base is marked by high-amplitude unconformity. Note steep normal faults which cut into flexed lithospheric plate, sometimes showing stratigraphic growth. Small number of faults propagate through contourite drift. Minor unconformity is visible toward top of contourite drift. Present-day moats within deeper trough are manifestations of current flow into and out of South Falkland Slope Drift. Migrating moats show encroachment of contourite drift to north. (b) Profile 3 is located ~200 km west of Profile 1. Drift is smaller with a larger amplitude, and its southern edge is now partly buried beneath trough sediments. Moat at northern edge of trough has evolved into a step. Diagenetic front is more clearly visible than on Profile 1. (c) Profile 5 is located ~200 km west of Profile 3 close to position where West Falkland Trough terminates. Drift is now barely visible beneath encroaching trough sediments. Trough itself is wider and shallower. Note extensive mud wave field which is generated by standing wave within water column. Diagenetic front is spectacularly imaged.

changes in bottom-water flow and should be an important source of ocean/climate proxies [*McCave and Hall*, 2006]. The stratigraphy of a drift is controlled by two related processes. The dominant external control is accumulation rate which is directly linked to changes in sediment supply and current activity [*McCave*, 2008]. Local processes (e.g., biological activity and water chemistry, both producing and dissolving sediment components) have a modulating effect.

[7] The stratigraphic architecture of a contourite drift is best determined from multi-channel seismic reflection profiles calibrated by well-log information. In the past, 3.5 kHz and single-channel or low-fold seismic surveying have been the principal tools although they are gradually being supplanted by industry-standard surveying which exploits long streamers, powerful airgun arrays and a high fold of cover. The resultant images are excellent, crisply defining both contourite shape and internal geometry. Contourite drifts have lenticular, convex-upward shapes. Internally, they have subparallel, moderate to low-amplitude reflections which change gradationally between seismic facies, revealing lateral migration of the sediment body caused by the interaction of a bottom current with morphology. In the southern hemisphere, the Coriolis force deflects slope-parallel currents to the left to produce up-slope deposition [*Faugères et al.*,

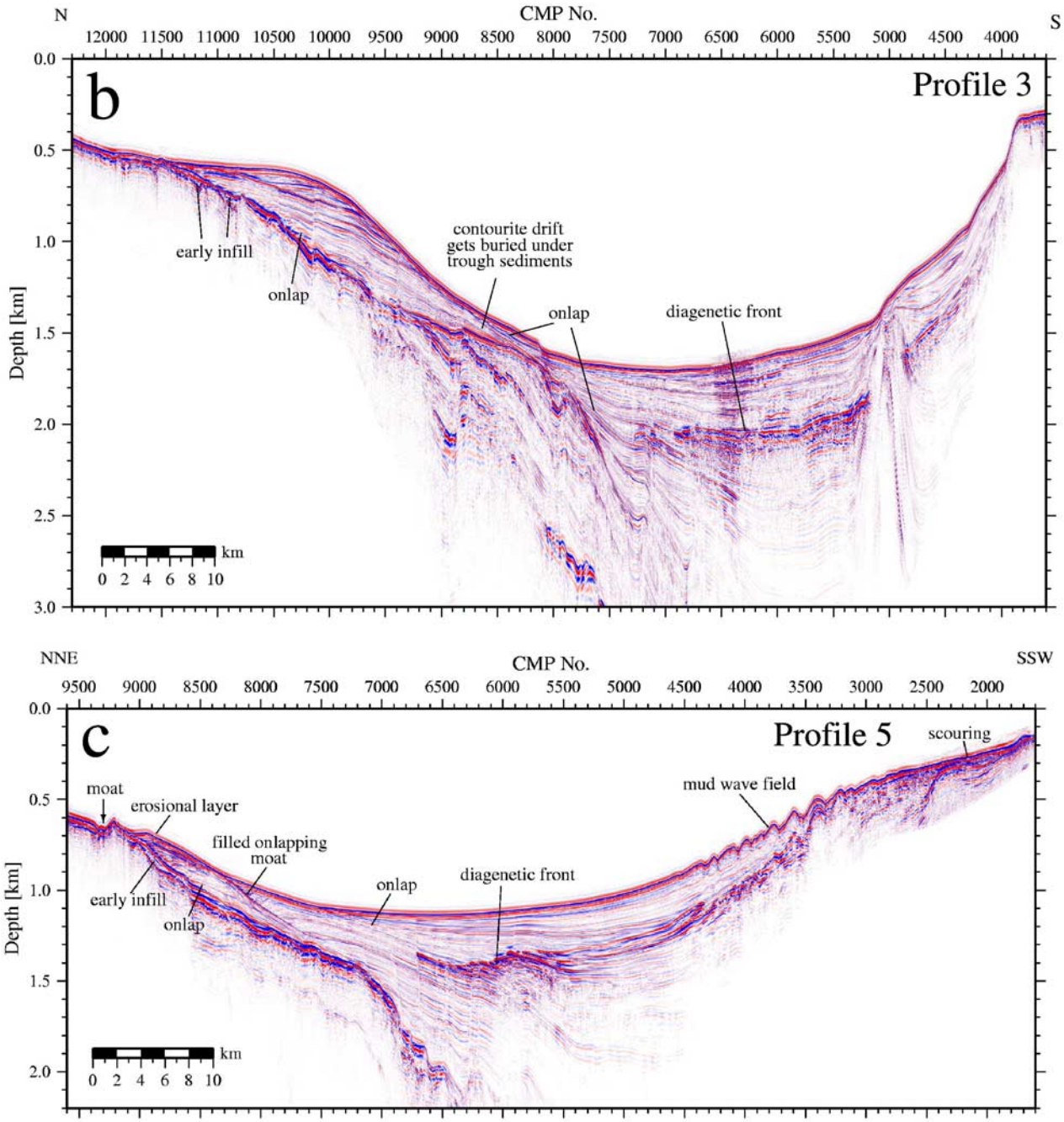

Figure 2. (continued)

1999]. Variations in bottom currents are responsible for deposition of mounded and sheeted drifts as well as for episodes of nondeposition or erosion which generate hiatuses. The internal reflectivity of a contourite drift depends upon acoustic velocity and density changes within the sedimentary pile. Thus mappable seismic reflections probably manifest changes related to phases of sedimentation separated by nondeposition or erosive events. Laterally continuous reflections represent periods when sediment supply or composition has varied or when current-controlled erosion occurs. Such events could have a climatic or a tectonic origin (e.g., opening/closing of sills and gateways which control bottom current flow). They have often been demonstrably linked to changes in seismic facies and serve as the basis for division of the drift into sediment packages [*Stow et al.*, 2002]. Less reflec-

tive packages between erosional events represent relatively stable bottom current regimes.

[8] Our purpose is threefold. First, high-quality seismic images with excellent signal penetration are used to describe the setting, morphology and internal structure of Neogene sedimentary drifts which occur within an important oceanographic gateway. Second, we have mapped the internal seismic stratigraphy of the SFSD and shown that the principal stratigraphic horizons record significant changes in oceanic circulation. Third, we suggest that this well-imaged contourite drift would make an excellent drilling target and that the grid of reprocessed seismic profiles constitutes a high-quality site survey.

2. Seismic Stratigraphy

[9] We have adopted the drift nomenclature proposed by *McCave and Tucholke* [1986] and *Faugères et al.* [1999]. Identification of contourites from sedimentary features alone is difficult because the slow and continuous nature of accumulation means that primary features can be masked or removed by secondary effects such as bioturbation [*Stow et al.*, 2002]. Accumulation rate is controlled by the intensity of the bottom current and by availability of terrigenous and biogenic sediment [*Faugères et al.*, 1993]. Drift geometries are grouped into four main classes on the basis of overall morphology: sheets, elongate mounds, channel-related drifts and confined drifts [*Stow et al.*, 1998]. The SFSD falls in the sheet category and is a "plastered drift" (i.e., it has a sheet-like form and is plastered onto a sloping continental margin [*Hollister et al.*, 1978]). In contrast, the West Falkland Trough Drift is a channel-related or confined drift.

2.1. Processing Strategy

[10] The grid of seismic reflection profiles shown in Figure 1 was acquired by Geco-Prakla (now WesternGeco) in 1993. The data are of excellent quality and have a record length of 9–12 seconds two-way traveltime. An airgun array consisting of 40 bolt guns, ranging in volumes from 30–500 cubic inches and with a total volume of 7288 cubic inches, was towed at an average depth of 7.5 m. This array was fired every 40 m at a pressure of 2000 psi. A 4780 m long streamer with 240 data channels, a near-trace offset of 92–97 m, and a 20 m group interval was towed at 10–10.4 m depth. The resultant fold of cover is 60 with a sampling rate of 2 ms. These data were acquired and processed in order to image the general structure of the South Falkland Trough. Although the contourite drift and trough deposits are clearly imaged on the original stacked sections, the original processing sequence was not designed to specifically target such shallow features.

[11] In order to generate higher-resolution images of the contourite drift, we have reprocessed field tapes of Profiles 1–5 at their original acquisition sample rate of 2 ms. The reprocessing sequence was specifically designed to enhance imaging of the first 3 s. Salient aspects of this sequence are source signature deconvolution, dense velocity analysis, source/receiver deghosting and post-stack migration. Source signature deconvolution was applied to shot records by using the recorded far-field source signature. This form of deterministic deconvolution does depend upon the exact repeatability of the airgun source. Inevitably, changes in source depth and sea state mean that the true source waveform varies through time. Nevertheless, in the absence of a far-field source signature for every shot, our limited application of deterministic deconvolution does successfully remove the bubble pulse and considerably reduce reverberation. A low-cut filter helped to reduce low-frequency noise which tends to be enhanced when the source signature is imperfectly known. Velocity analyses were carried out every 2 km. Deghosting was applied after normal move-out correction and standard multiple energy suppression by assuming a constant source/receiver depth and a flat sea surface. This simplified procedure was successful in further compressing the source signal and reducing ringing. A standard spherical divergence correction was used to remove amplitude transmission losses but otherwise no automatic gain control was applied and so the seismic images are shown at true amplitude. Finally, we did not attempt to carry out prestack depth migration since structural dips and velocity contrasts are modest. Instead, a Stolt *f-k* time migration with a constant velocity of 1500 m/s was applied down to the water-bottom multiple where a bottom mute function was set. Before the data were transformed into the Fourier domain, vertical stretching was applied to allow for vertical changes in velocity. This simple migration algorithm successfully removed all significant diffraction events.

[12] We present both time and depth-converted profiles. Before depth conversion, a static correction of +12 ms was added to compensate for source

Table 1. Interval Velocities and Standard Deviations of Individual Depositional Units

Contourite Layer	Interval Velocity, m/s	Maximum Depth, m
Unit 2B	1512 ± 8.4	59
Unit 2A	1516 ± 11.4	129
Unit 1B	1608 ± 17.9	327
Unit 1A	1758 ± 14.8	522

and receiver depth. Time-to-depth conversion was carried out using the picked root-mean-squared (RMS) velocities and lateral variations were taken into account by averaging velocities within a given sedimentary sequence. Table 1 shows the interval velocities assigned to the different sequences. These velocity values agree with commonly assumed values. For example, *Howe and Pudsey* [1999] assumed a maximal acoustic velocity of 2000 m/s for contourite deposits in the northern Scotia Sea and *Howe et al.* [1994] assumed velocities of 1550 m/s for a contourite drift in the northern Rockall Trough. Our method is simple and approximate but it is reasonable in the absence of borehole information.

[13] The reprocessed images are shown in Figures 2–7 and 12–14. Signal penetration and vertical resolution are excellent, demonstrating the value of using industry-standard acquisition combined with a processing sequence which was specifically designed to enhance shallow sedimentary structures.

2.2. South Falkland Slope Drift

[14] Stratigraphic mapping was carried out on the reprocessed versions of Profiles 1–5 which are approximately dip lines crossing the South Falkland Trough. Previously processed versions of Profiles 6–9, which are roughly parallel to the strike of the basin, were used to provide additional constraints. These cross lines were resampled at 4 ms during the original processing and have not been depth-converted. Profiles 1–5 and 6–9 do not exactly tie since different post-stack time migration algorithms were used (Stolt and *f-x* algorithms, respectively). Figure 2a shows three representative north-south profiles which illustrate the structural context of contourite drift and trough deposits. The contourite drift is clearly visible on Profiles 1 and 3 (Figures 2a and 2b) where it sits on top of truncated and normally faulted Mesozoic sedimentary rocks which constitute the flexed northern flank of the South Falkland Trough [*Bry et al.*, 2004]. It is less obvious on the westernmost line, Profile 5, where it is much reduced and partially obscured by onlapping trough deposits. Where the contourite drift is thickest, it consists of a regular stack of clearly mappable reflections, several of which are very prominent (Figure 2a). This stratigraphic pile has been slightly disrupted by a series of steep normal faults which cut into the flexed plate beneath. One obvious unconformity occurs close to the top of the contourite drift (Figure 2b).

[15] Close-ups of the SFSD have been used to map its internal stratigraphy (Figures 3–7). The drift thickens and widens toward the northeast, taking the form of a thin plastered sheet. Water-depth changes from 650–1100 m along the westernmost profile to a range of 400–2000 m further east (compare Figures 3 and 7). Lenticular, symmetric and asymmetric depositional units separated by continuous reflections which onlap and downlap onto an irregular basal discontinuity can be identified. This basal discontinuity dips southward and it is usually a major unconformity. Between Mesozoic basement and unconformity, a sporadic, early sedimentary infill can be recognized. Occasional incisions indicate the existence of erosive channels (e.g., Figure 6). Minor normal faults, which dissect the drift, are caused by downwarping of the northern margin of the Falkland Trough. Some of these faults break the sea bed or have demonstrable stratigraphic growth which shows that normal faulting occurred during drift deposition. On Profiles 1 and 2, aggradational and progradational packages accompanied by thinning toward the drift margins are observed and the entire contourite drift body is more or less symmetrical. From Profile 3 westward, however, the crest of the drift migrates northward until it is at the northern end of the contourite drift on Profile 5 (Figure 7). The uppermost sediments are separated from the main contourite drift body by a prominent unconformity.

[16] One might expect to have contourite drift accumulations on both flanks of the South Falkland Trough and within the deeper part of the trough. There is a confined drift within the trough which grows eastward as identified by *Cunningham and Barker* [1996] and by *Howe et al.* [1997]. However, a plastered drift has only grown on the northern flank of the trough, probably because the southern flank is steeper. Erosive features such as moats are more common in the south.

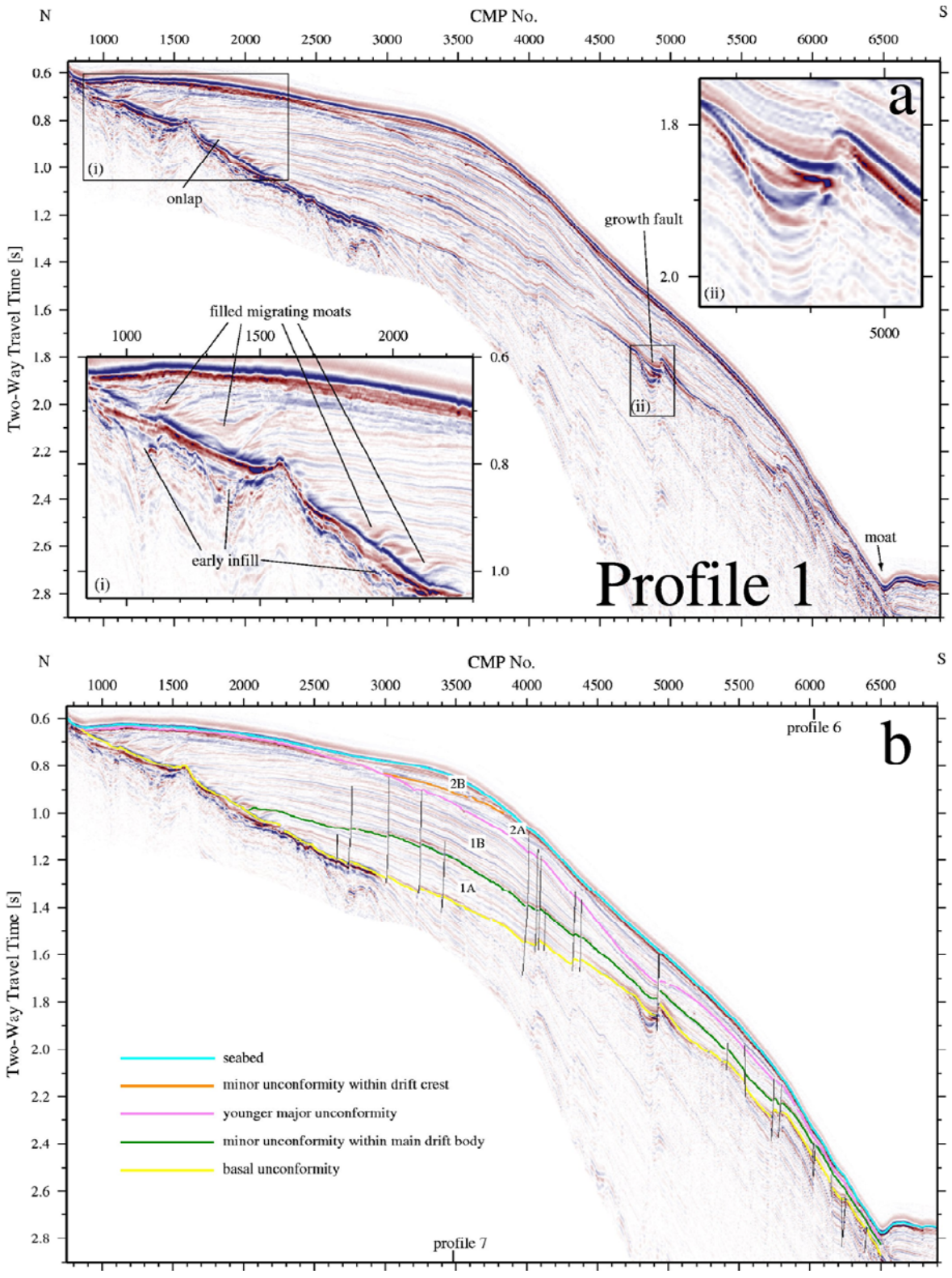

Figure 3. Profile 1. (a) Uninterpreted close-up of northern portion of Figure 2a, which best illustrates internal stratigraphy of contourite drift which takes form of thin plastered sheet. Mappable units within drift together with its sharply defined base are clearly visible. Inset i is a detail which shows early fill of rugged preexisting topography and filled migrating and onlapping moats. Inset ii is a detail which shows normal fault across which stratigraphic growth has occurred. (b) Interpreted version which shows mapped horizons, delineating 4 sedimentary packages, and normal faulting.

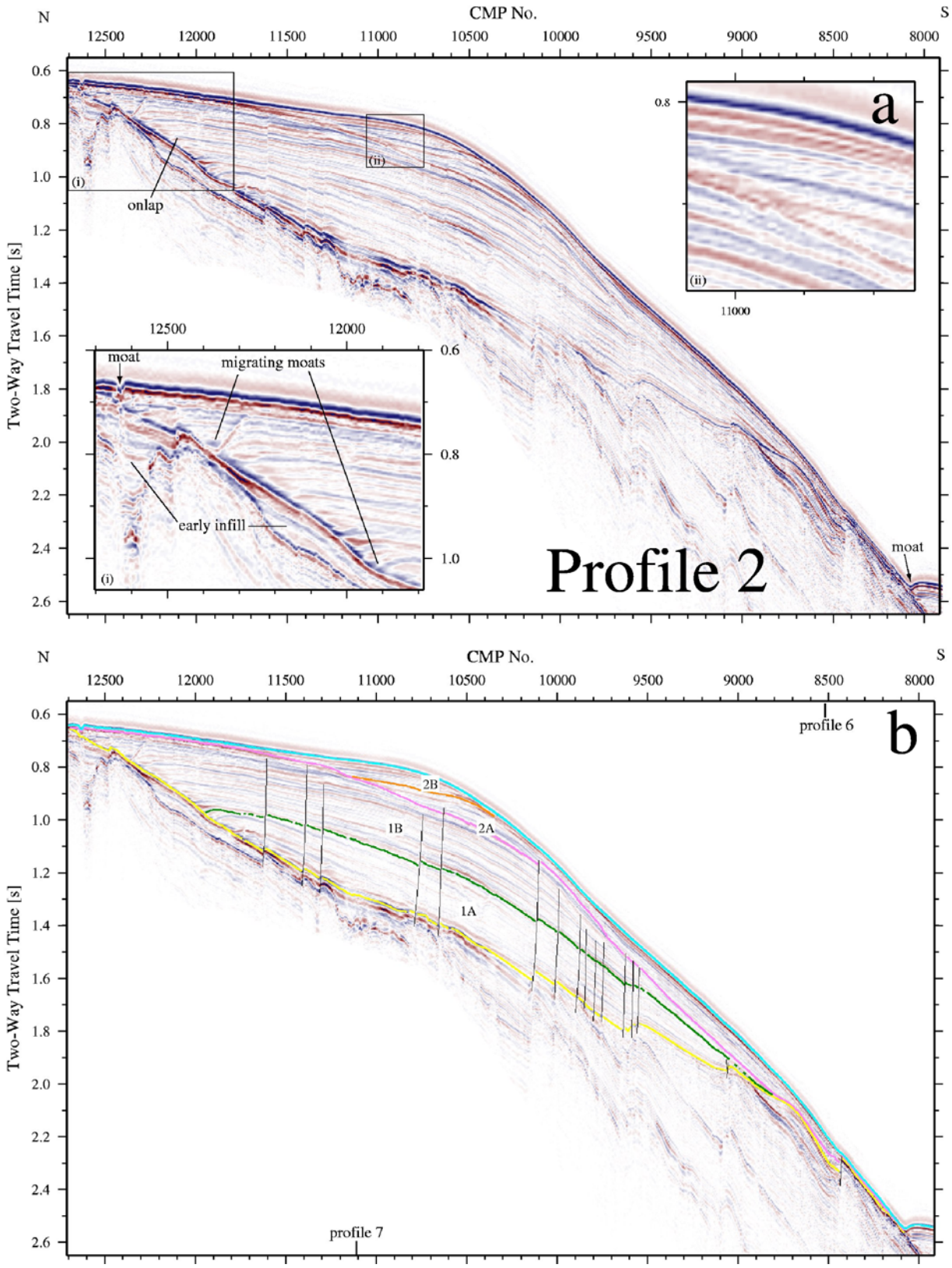

Figure 4. Profile 2. (a) Uninterpreted close-up of northern portion which also clearly illustrates internal stratigraphy of symmetric contourite drift. Inset i is a detail which more clearly shows preexisting topography, including channel structure, and several migrating moats. Inset ii is a detail which shows onlapping stratigraphy above youngest unconformity. (b) Interpreted version which shows mapped horizons and normal faulting.

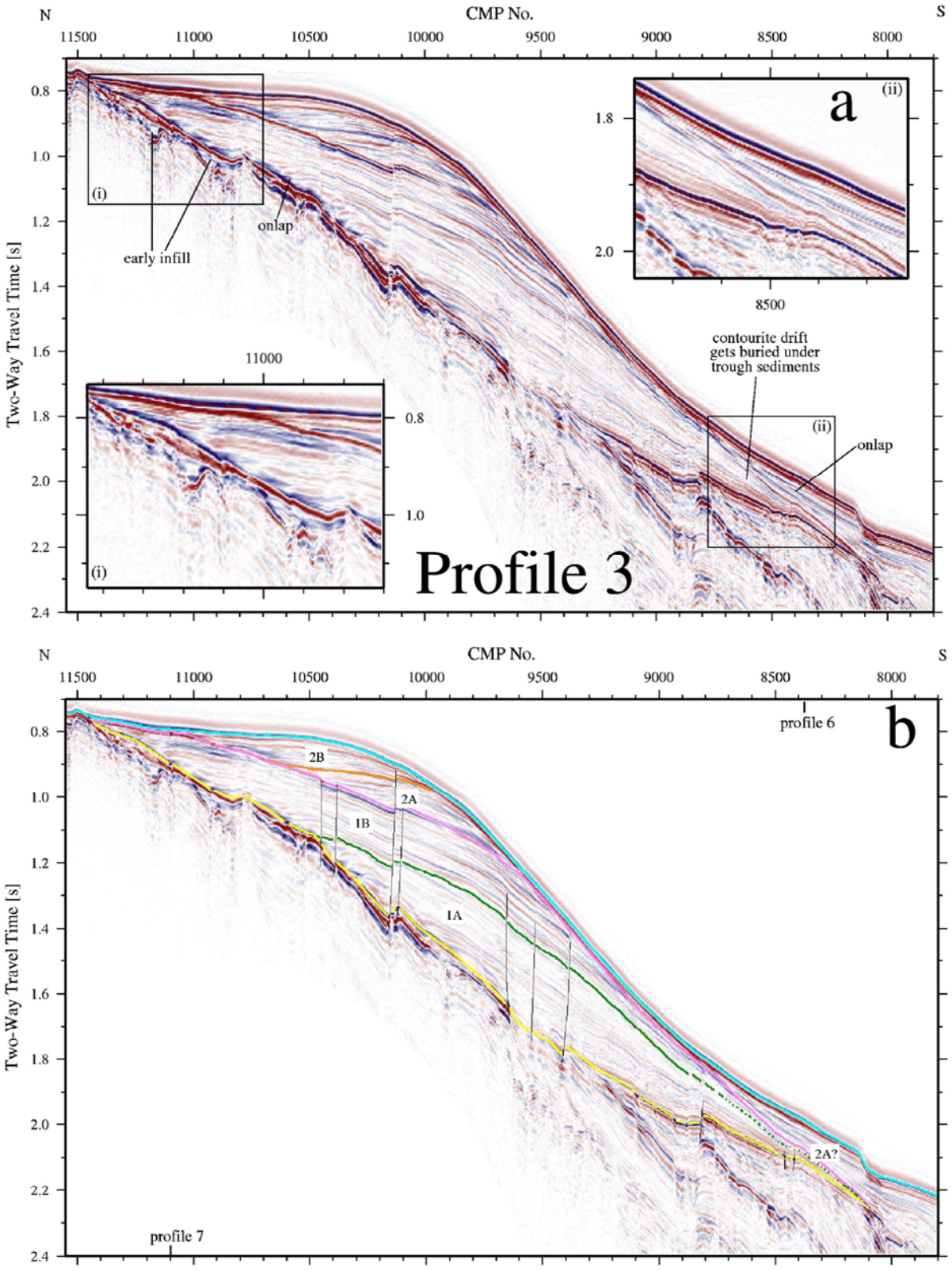

Figure 5. Profile 3. (a) Uninterpreted close-up of northern portion of Figure 2b showing smaller drift which is partly buried beneath trough sediments. Crest of drift is migrating up onto shelf. Note stratigraphic continuity with previous profiles but smaller number of normal faults. Inset i is a detail showing the way in which preexisting topography is sometimes fault-controlled. Inset ii is a detail which shows encroachment of trough sediments onto southern edge of contourite drift. (b) Interpreted version which shows mapped horizons and normal faulting.

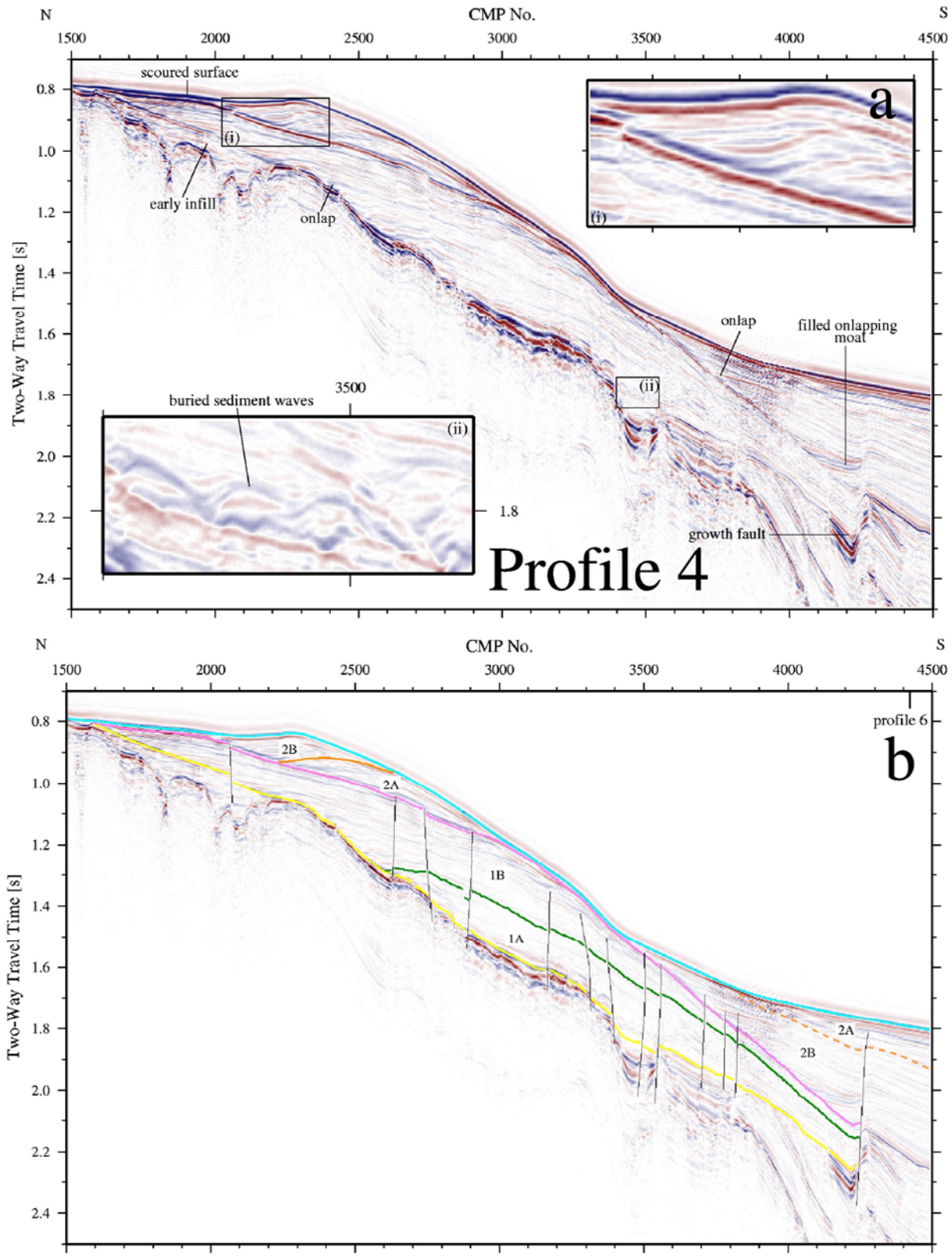

Figure 6. Profile 4. (a) Uninterpreted close-up of northern portion. Note marked difference with eastern profiles: contourite drift is partly buried and reduced in extent, while youngest unconformity surface is strongly reflective. Inset i is a detail showing structure of contourite drift above youngest unconformity. Note migration of crest. Inset ii is a detail showing buried sediment waves within lowest stratigraphic unit. (b) Interpreted version which shows mapped horizons and normal faulting.

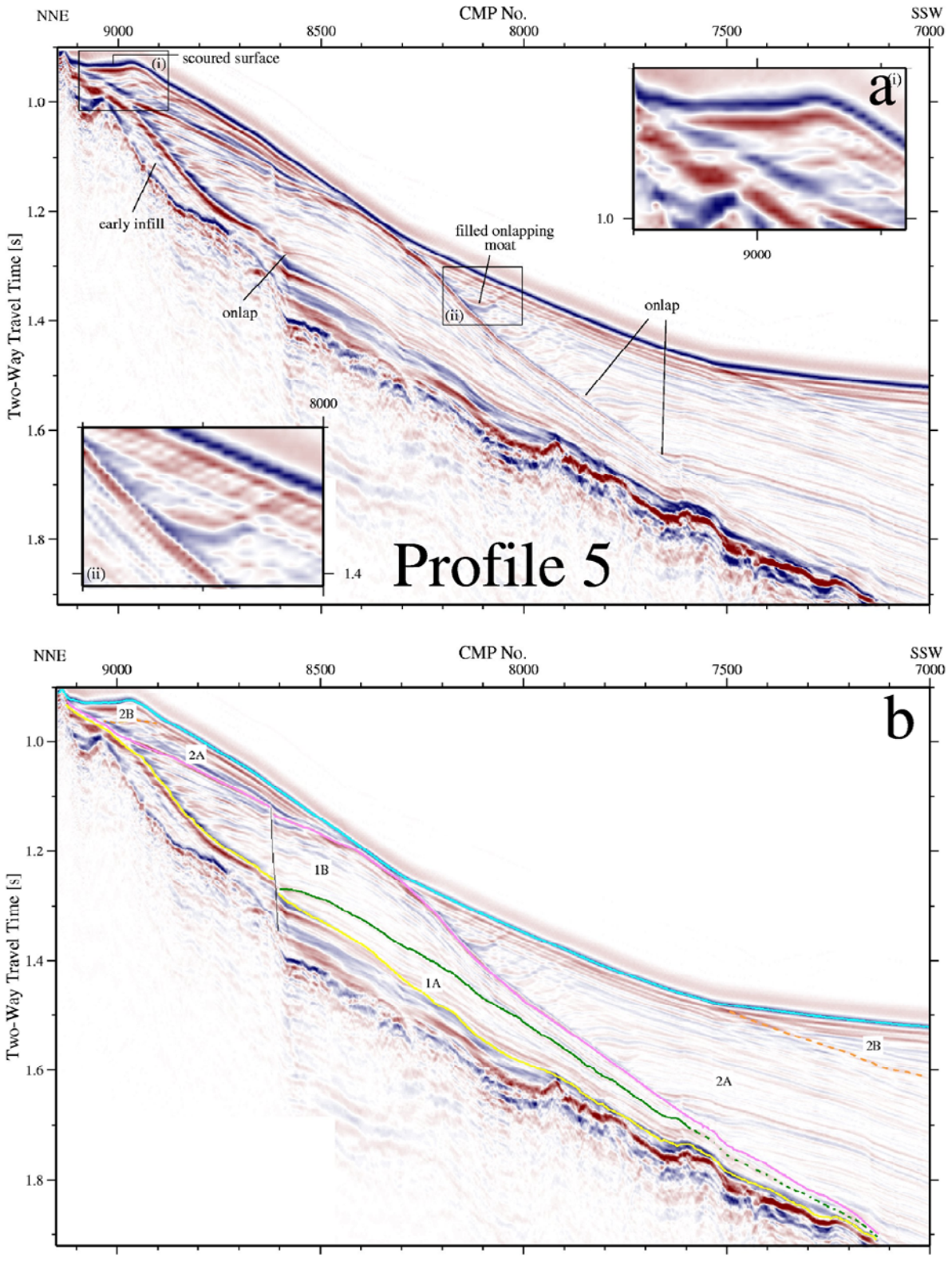

Figure 7. Profile 5. (a) Uninterpreted close-up of northern portion of Figure 2c. This westernmost profile crosses wide and shallow end of trough where contourite drift is much diminished and almost completely buried by trough sediments. Early fill is more extensively developed, and its top is marked by a bright reflection. Upper portion of contourite drift is migrating northward. Inset i is a detail showing structure of contourite drift above youngest unconformity. Inset ii is a detail showing filled onlapping moat within trough sediments. (b) Interpreted version which shows mapped horizons.

2.3. Major Sedimentary Sequences

[17] We have used the seismic reflective character of the SFSD to identify and map four surfaces. Inspection of Profiles 1–5 suggests that there are several prominent internal reflections which can be used to subdivide the drift. The basal unconformity (yellow horizon) is eminently mappable and represents the bottom of the drift. Initiation of drift accretion could have been a response to a decrease and/or a reorientation of current activity. The younger main unconformity (magenta horizon separating Units 1 and 2) is defined by truncation of reflections and is caused by erosion and redeposition of sediments. This surface is represented by a relatively strong reflection which is often close to, and thus sometimes hard to distinguish from, the sea bed (Figure 7). In between these two major unconformities, a strong reflection (green horizon) can be identified delineating a change in seismic facies from the more transparent lower sedimentary sequence (Unit 1A) to a more reflective seismic facies (Unit 1B). The youngest package above the younger unconformity (magenta horizon) can also be divided into two sequences (Units 2A and 2B) by another strong reflection (orange horizon), separating a regular and a more chaotic sequence (e.g., Figure 5). This reflection is scarcely identifiable on Profile 5. Since the SFSD thins considerably to the south, it is not possible to trace this unit on Profile 6, so that the thickness of sediment between the younger unconformity and the sea bed is unknown.

[18] Unit 1A is weakly reflective to acoustically transparent, which suggests that deposition was continuous and homogeneous, implying low to moderate bottom current velocities of $\leq$10 cm/s. Generally, reflections within this sequence onlap and downlap onto the basal unconformity (Figure 8). On dip profiles, this lowest sequence appears to be more or less symmetrical. This symmetry is clearly evident on the isopach map (Figure 10). Two minor anomalies interrupt the smooth variation in thickness across and along the unit. The most striking one is related to a deep V-shaped channel structure seen on Profile 6 (Figure 11). It is located at CMPs 8600–9400 between Profiles 2 and 3, close to the base of the northern slope where moat-like structures occur. This channel incises into sediments beneath the drift to a depth of 568 ms (i.e., 500 m) and it has a maximal width of about 8 km. It is the deepest feature on the seismic profiles and was almost certainly cut by turbidity currents. Another channel structure was identified within the sedimentary sequence on Profile 2 at CMP 12500 (see inset of Figure 4). A second anomaly, on a much smaller scale, is found on the same line at CMP 11500–14100 and has the shape of a basin: it is 26 km across but only 130 ms (i.e., $\sim$115 m) deep. It is probably drift fill of preexisting rough topography. Slightly stronger current activity during the earliest times can also be deduced from the buried sedimentary waves observed on Profile 4 (see inset of Figure 6). Similar features occur at the base of the slope above an old channel incision in an underlying sedimentary sequence of possible Paleogene age. Unit 1A peters out toward the northeast. On Profile 9, it is already thin and on Profile 8 it is completely absent. The overall orientation of the drift axis reflects flow distribution along the slope. Along axis, current flow slowly promoted growth whereas at the drift margins, flow was intensified and only thin deposits and erosive features (e.g., depressions, moats) are found. The current axis followed the slope around from more or less W–E, changing to SW–NE at the eastern end.

[19] Unit 1B is the thickest package and has strong internal layering. This seismic facies is indicative of abundant hiatuses and periods of condensed sedimentation which are probably linked to increased bottom current intensity. It suggests episodic sedimentation with more variability in either current velocity or sediment supply or both [*Stow et al.*, 2002]. On Profiles 4 and 5, this seismic facies becomes more transparent suggesting more uniform deposition in the west. On all lines except Profile 6 where sediment cover is very thin, reflections within this sequence onlap onto both the unit beneath and, up dip, onto the basal unconformity. Deposition within the unit is thus asymmetric and migrates upslope. This migration is confirmed by the filled moats which are generated when onlapping surfaces migrate upslope. These collective observations clearly illustrate growth of the drift (see, for example, insets of Figures 3 and 4). Maximal thickness of this sequence is 332 ms (267 m) with a depocenter on Profile 8 (Figures 9 and 10).

[20] A dramatic change occurs at the boundary between Units 1B and 2A. Overall, Unit 2 is thinner and of much lesser extent than Unit 1. This change reflects either reduced sediment supply or stronger ACC flow. Unit 2A is much smaller than Units 1A and 1B. The reduction is especially clear in the western part where only a very thin sediment cover remains. The maximal thickness is 148 ms (113 m). Internally, Unit 2A's reflections onlap and

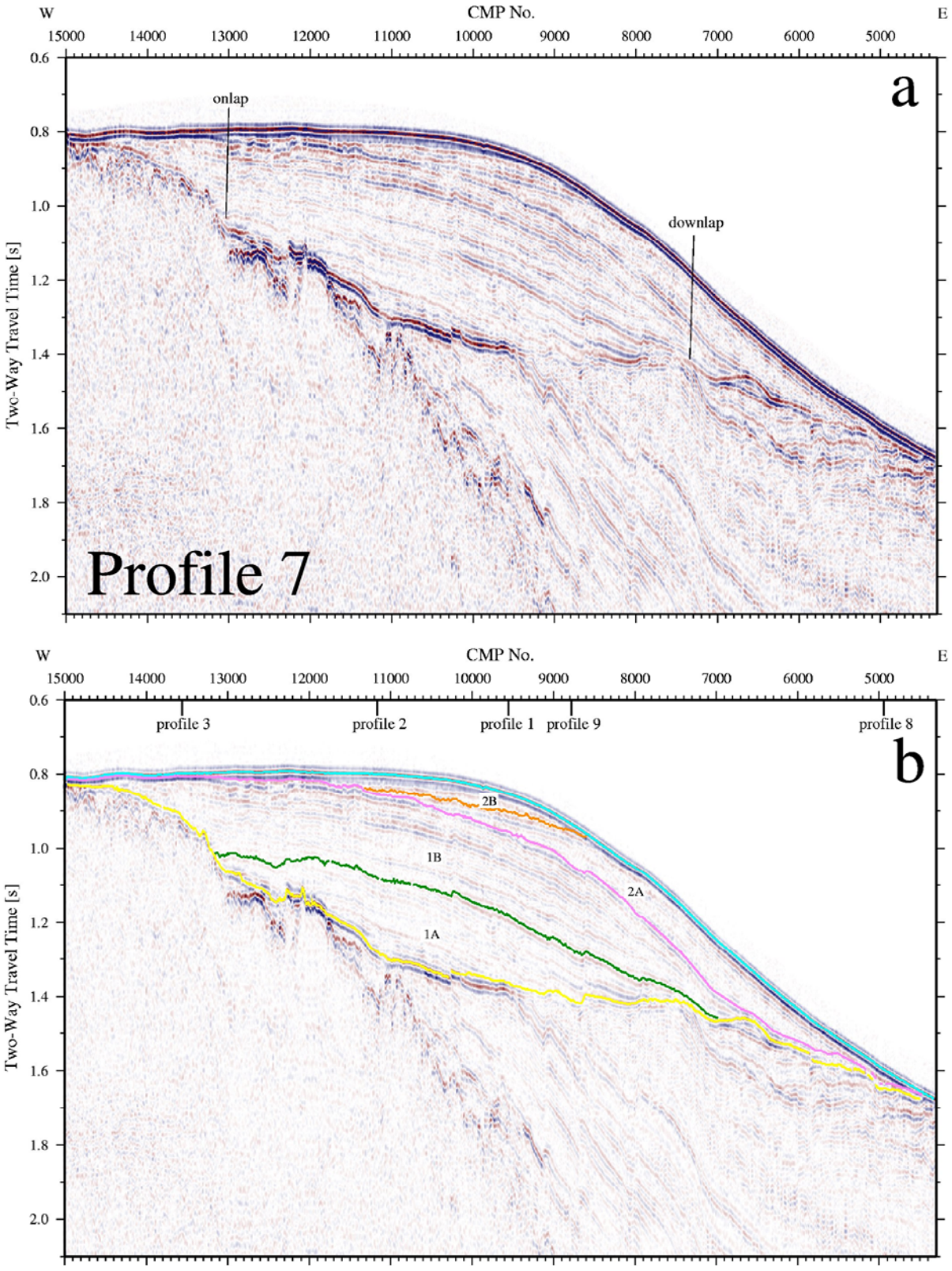

Figure 8. Profile 7 was not reprocessed at 2 ms and does not reveal as much detail. (a) Uninterpreted close-up of central portion. This east-west profile crosses northern edge of trough where contourite drift is thickest and it illustrates how contourite drift migrated during its growth. Oldest part of drift is acoustically transparent. Base of drift is clearly visible, especially between CDPs 10000 and 13000. Note that internal stratigraphy can still be correlated with dip profiles. (b) Interpreted version which shows mapped horizons.

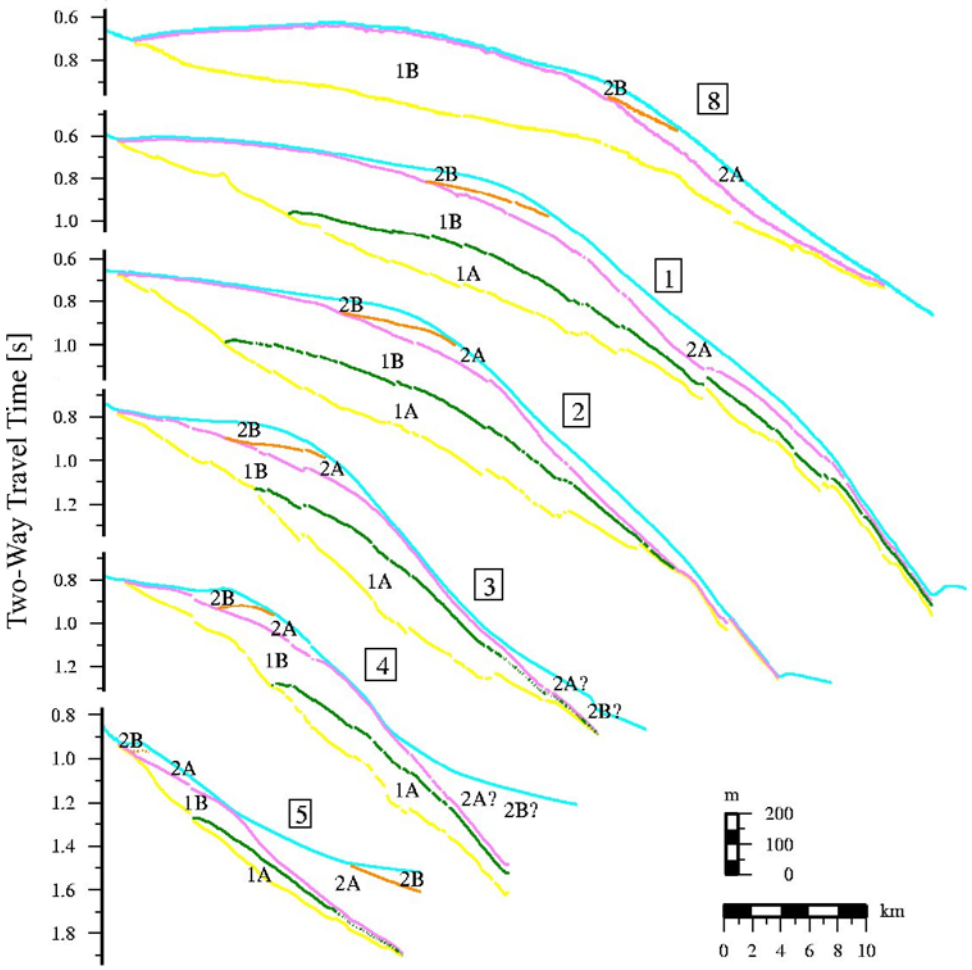

Figure 9. Stacked line drawings of mapped reflections which divide contourite drift into 4 units. Numbered boxes, profile numbers; yellow and pink lines, basal unconformity and youngest unconformity, respectively; green and orange lines, prominent and mappable internal reflections; blue line, seabed. Two-way traveltime and depth scales are shown.

partly downlap onto the underlying unconformity and they are truncated at the sea bed. The seismic facies character varies from more reflective to more transparent (compare Figures 3 and 6). The depositional axis suggests a nearly W–E current direction.

[21] Finally, Unit 2B is dominated by subparallel, more diffuse and chaotic seismic facies which indicates intensified bottom current activity (flow speeds of 12–20 cm/s according to Figure 8 of *McCave and Hall* [2006]) and possibly a significant decrease in sediment supply (e.g., Figures 6 and 7). Progressive onlap of subparallel laterally continuous reflections with high amplitudes suggest an upslope (northward) prograding pattern. Internal reflections are truncated at the unconformity and at the sea bed. More westerly profiles show that the northern margin of the plastered drift underwent peripheral scouring which caused erosional truncation. Sediment thickness is considerably reduced to a maximum of 95 ms (72 m).

[22] Figures 9 and 10 summarize the stratigraphic growth of the SFSD, which covers about 5500 km^2. The only significant anomalies are caused by channel incisions along its southern perimeter. The inferred direction of the current tracks the bathymetry and is similar to the present-day flow of the ACC: approximately W–E but tending to SW–NE at the flared, eastern end of the trough.

2.4. West Falkland Trough Infill

[23] Deposits within the South Falkland Trough were formed from sediments predominantly transported by turbidity currents. These currents probably came from the west, north, and possibly south.

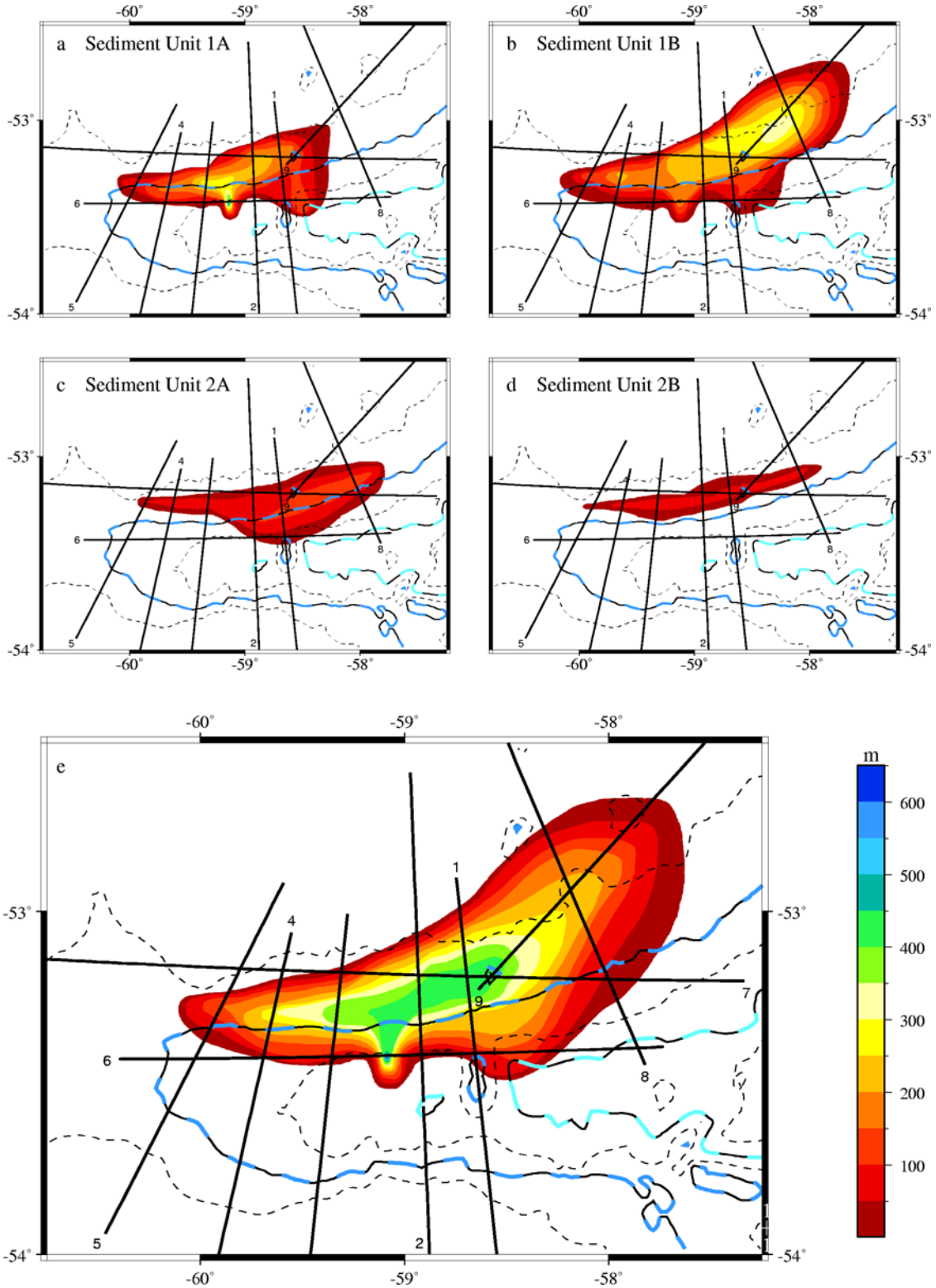

Figure 10. Set of isopach maps which show thickness of each mapped unit and total thickness of contourite drift. Numbered black lines, profiles used to map drift; dark and light blue dashed lines, 1000 m and 2000 m bathymetric contours, respectively; dashed lines, other bathymetric contours. Note lobate shape of contourite drift and short wavelength lobes which indicate north-south channels along northern edge of trough.

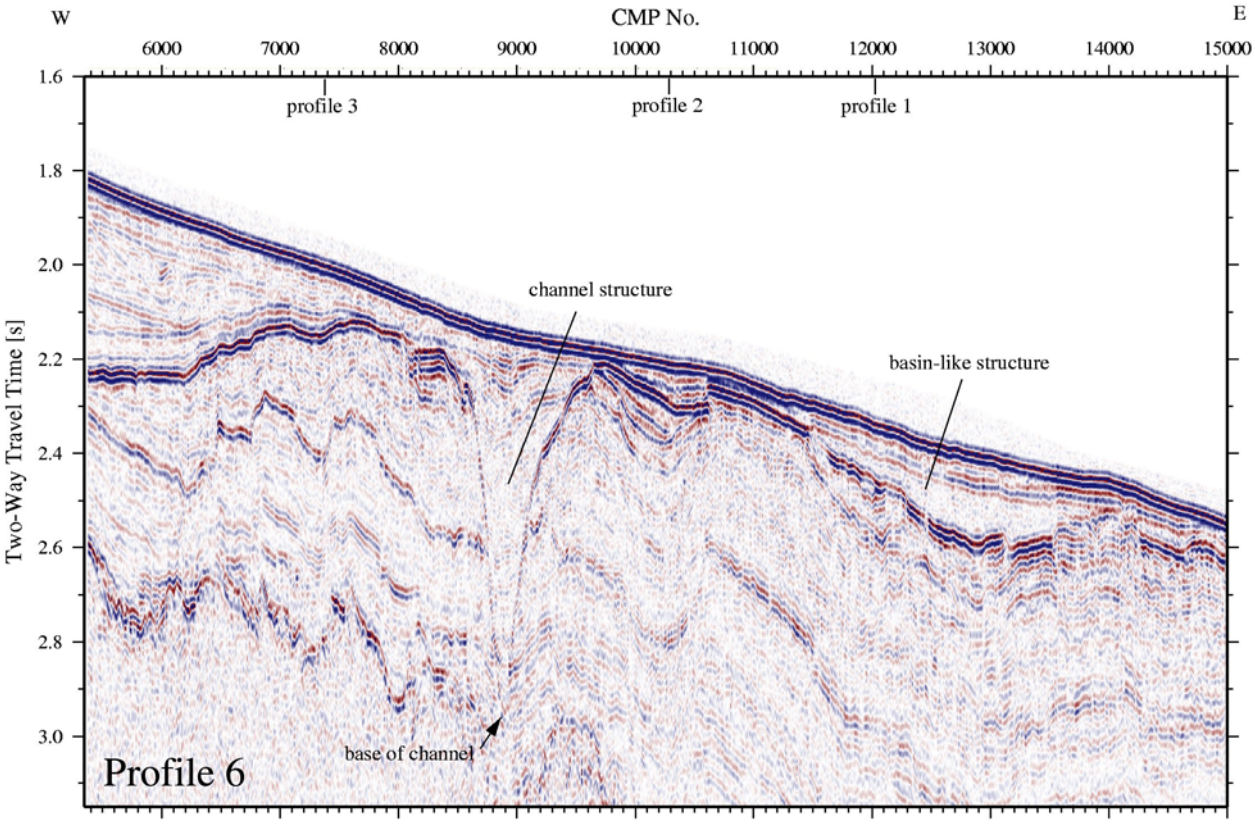

Figure 11. Uninterpreted close-up of central portion of Profile 6 which was not reprocessed at 2 ms and does not reveal as much detail. This east-west profile runs along northern margin of trough close to base of contourite drift where it is almost completely buried by trough sediments. Most striking feature is narrow, filled channel which is 748 ms (i.e., ~624 m) deep. This channel is clearly visible on isopach maps (Figure 10). Note significant growth across normal fault at CDP 10500.

Further east (i.e., downslope), *Cunningham et al.* [2002] have interpreted similar deposits as a confined drift. In the upslope region, we expect significant downslope sediment transport, and indeed the seismic facies of the trough fill comprises packets of high-amplitude reflections which are more typical of turbidites, which tend to have strong lithological contrasts, than of contourites which are dominated by muds.

[24] On Profile 1 (Figure 2a), the deposit is slightly mounded which agrees with *Cunningham et al.* [2002], who show that it has become a confined drift by 56° 30′ W. We have not attempted a detailed breakdown of the stratigraphy. Nevertheless, the excellent acoustic images displayed in Figures 12–14 are worthy of examination. A dominant feature of part of the trough are bright, time-transgressive reflections cross-cutting primary sedimentary strata (see especially Figure 14). These bright reflections occur throughout the South Falkland Trough but they are more clearly developed at the western end where they are compartmentalized by steep normal faults. They represent strong acoustic impedance contrasts which absorb most of the transmitted seismic signal and, as a result, underlying strata are much more weakly imaged. Without borehole control, the origin of these features remains uncertain. However, we do not believe that they represent gas-filled layers and they are probably too deep to be clathrate deposits. The most likely cause is silica diagenesis from opal-A to opal-CT which can generate changes in lithification which give rise to strong impedance changes [e.g., *Davies*, 2005]. Similar features have been observed on multi-channel seismic reflection data from the eastern Falkland Trough by *Cunningham et al.* [2002]. *Carter and McCave* [1994] and *Carter et al.* [2004] identified a reflection within the North Chatham Drift, initially thought to be a proto-drift but which subsequent drilling on ODP leg 181 (site 1123) has shown to be a diagenetic front.

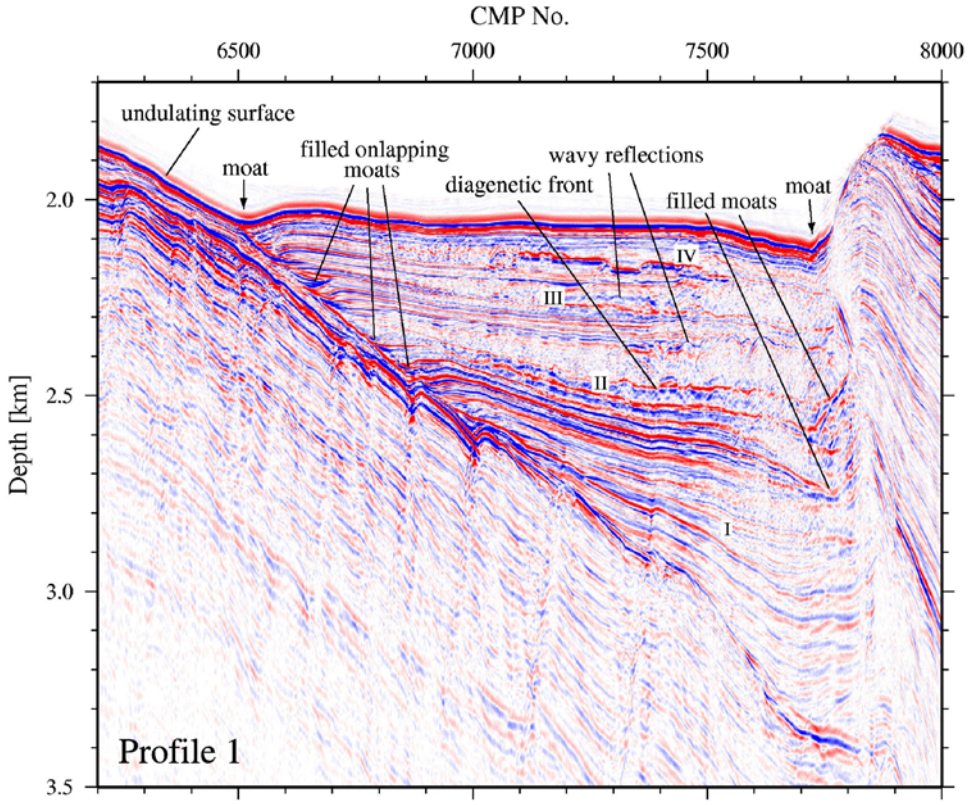

Figure 12. Profile 1. Uninterpreted close-up of southern portion which shows internal stratigraphy of trough deposits south of contourite drift. Note base of triangular-shaped foreland basin which sits on top of flexed and normally faulted crust. Dense array of normal faults show evidence of stratigraphic growth and sometimes penetrate into basal sediments of the foreland basin. Stratigraphy within trough is rich with detail: note, for example, evidence for diagenetic front and for filled onlapping moats at northern and southern edges. Roman numerals are broadly indicative of four different stratigraphic patterns: I, well-bedded, mappable strata which show stratigraphic growth; II, parallel-bedded, mappable strata; III, mixture of continuous and wavy bedded strata which show effects of diagenesis; IV, youngest, poorly bedded strata.

[25] Profiles 1, 2 and 5 illustrate how the internal stratigraphy of the West Falkland Trough evolves as the trough itself shallows markedly from east to west (Figures 12–14). On Profile 1, the trough fill clearly forms a triangular wedge which represents foreland basin subsidence. This accommodation space was generated by thrust loading of the Falkland Plateau: the frontal, active thrust fault is clearly observed and the flexed Falkland Plateau is cut by closely spaced, steep normal faults (Figure 12). At the sea bed, two moats occur on either side of the trough and bathymetry is similar to that described by *Cunningham et al.* [2002] from seismic profiles located further east but without the clearly mounded drift. This moat configuration suggested to them that the trough fill was a confined drift deposit. These moats are less distinctive on Profile 3 where they are reduced to steps on the southern side of the trough. Sea-bed moats are no longer visible on Profile 4. This moat evolution is consistent with looping of bottom currents which flow clockwise around the western end of of the trough beneath the SAF.

[26] The trough fill is an important record of foreland basin evolution as well as bottom current activity. However, SFSD stratigraphic mapping cannot be easily extended into the trough itself, partly because of stratigraphic condensation and partly because trough sedimentation was dominated by turbidity currents unrelated to current activity. The chief source of trough sediment is probably terrigenous material transported axially from southern South America while some material may have been supplied from Burdwood Bank and from the Falkland Plateau. We have roughly divided the fill into four stratigraphic sequences, Units I–IV (Figures 12–14). Unit I is wedge-shaped and sits unconformably against tilted and faulted Mesozoic strata. The seismic facies is generally transparent

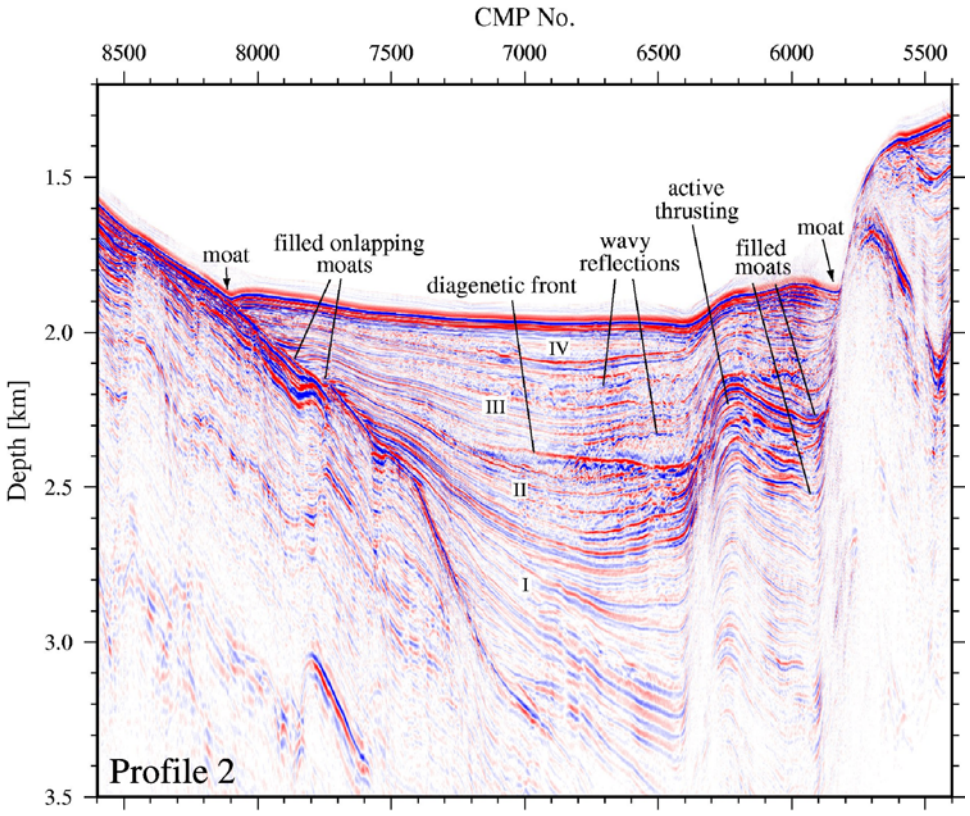

Figure 13. Profile 2. Uninterpreted close-up of southern portion which shows internal stratigraphy of trough deposits south of contourite drift. Compare with Profile 1. Note changed shape of base of foreland basin and of structure along southern margin. Diagenetic front clearly transgresses sedimentary architecture. Note evolution of moat structure through space and time.

with several bright and continuous reflections. There is overall stratigraphic growth toward the active plate margin with occasional prominent unconformities which demonstrates that Unit I was deposited during active plate bending when foreland subsidence commenced. On Profile 1 (Figure 12), normal faults penetrate into Unit I with stratigraphic growth which shows that flexing of the plate continued during infilling. Further west, Unit I becomes more deformed along the southern boundary of the trough (Figure 13). There is little evidence for moat formation within Unit I although isolated channels are occasionally visible. This absence suggests that this unit predates Unit 1A of the drift sequence when currents must have been active.

[27] The overlying Unit II has a sag-like appearance with more continuous and closely spaced reflections. On Profile 1, this unit is partially obscured by diagenetic effects although it is more clearly visible on Profile 2 where there is a single, discrete diagenetic front. Unit II is much less affected by normal faulting, especially on Profile 1. Stratigraphic growth is also much diminished which suggests that the rate of foreland subsidence has decreased. The northern and southern edges of Unit II are characterized by a series of pronounced moats which are best seen on Profile 1 and much diminished on Profiles 2 and 5, especially along the southern margin. These moats continue into the overlying strata. The seismic facies of Unit III consists of a mixture of continuous and wavy reflections with a partly transparent character. The succeeding Unit IV is rather similar in character. Neither unit shows much evidence for stratigraphic growth against the active boundary, which suggests that deformation along this boundary became predominantly strike-slip during deposition of these units. At the eastern end of the trough, Units III and IV are parallel to each other and conformable with underlying units. At the northern margin of the trough, all four units onlap the trailing edge of the SFSD. This geometry changes further west where Units III and IV onlap the top of the lower units and thicken to the south (e.g.,

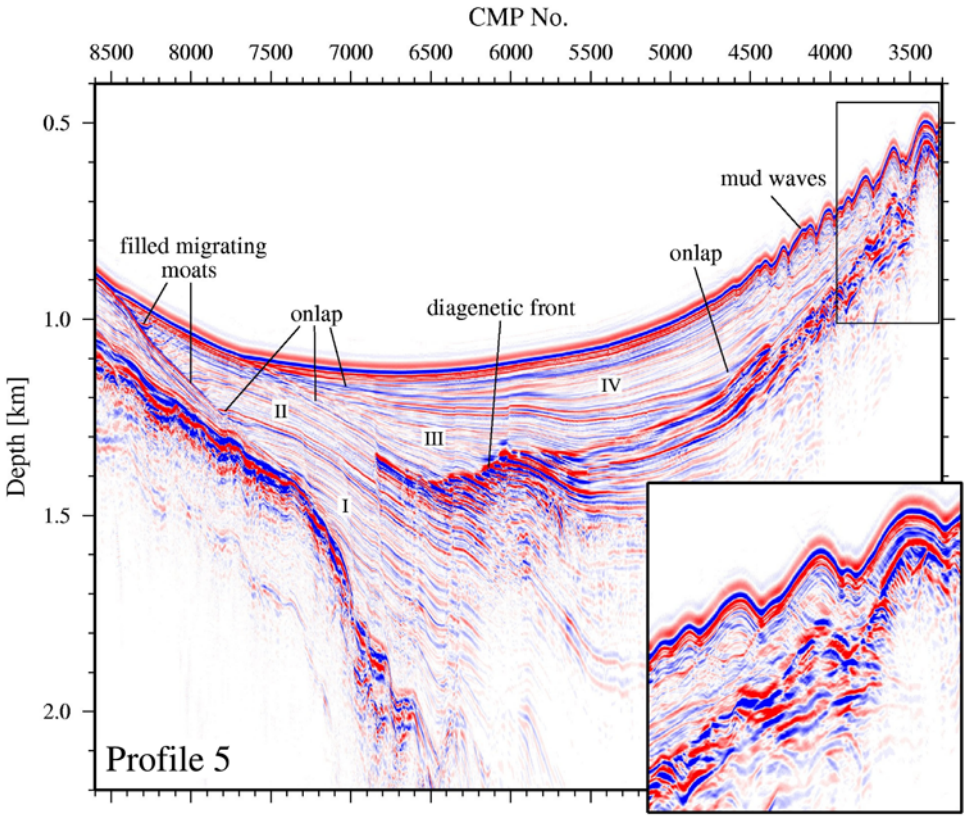

Figure 14. Profile 5. Uninterpreted close-up of southern portion which shows internal stratigraphy of trough deposits south of contourite drift. Compare with Profiles 1 and 2. Thrust faulting is less evident along southern margin where a field of mud waves occur. Filled onlapping moats are clearly visible at northern margin and show the way in which trough grew. Sedimentary Unit II is exposed at surface, and Unit III onlaps unconformity between Units II and III. Diagenetic front cuts across depositional units and is clearly fault-controlled. Inset shows detail of mud wave field. Note amplitude, asymmetry, and upslope migration of these sinusoidal waves.

Figure 14). This change is associated with the abrupt disappearance of moat structures which are present in Units II on Profile 5 and is probably related to a local decrease in current speed at the western end of the trough. This decrease is caused by a deepening of the flow as Unit II pinches out below ~1200 m. Burial of the trailing edge of the South Falkland Trough gives the relative ages of Units I–IV. Unit I must predate Unit 1A of the SFSD. We suggest that Unit II broadly correlates with Unit 1A of the SFSD and that Units III and IV correlate with Unit 2B.

2.4.1. Migrating Waves

[28] In the middle of the southern slope on Profile 4 (Figure 6) and on Profile 5 (Figures 2c and 14), aggradational stacks of depositional units comprising a field of small sedimentary waves are visible. These waves are sinusoidal but asymmetric, with internal reflection geometries which indicate upslope migration. They vary considerably in size. On Profile 5, the wave-like character of the seabed could be mistaken for creep although the sense of asymmetry does not favor this explanation. Where wave morphology is distinctive, the pattern is probably generated by a field of small mud waves. There are different scales of waves: while the smallest waves are approximately 500 m long and about 25 m high, the larger waves have a wavelength of 2 km and a maximal peak-to-trough height of 120 m. Underlying sediments have conspicuous wavy reflections at depths of 100 and 150 m on Profiles 4 and 5, respectively. On Profile 5, deeper mounded geometries at CMP 4050–4350 and a depth of 1200 m and at CMP 3500–3750 and a depth of 900 m indicate the existence of an older buried train of these migrating bedforms (Figure 14). Mud waves are commonly associated with bottom current activity on contourite drifts [*Flood*, 1988; *McCave and Tucholke*, 1986; *Faugères et al.*, 1999]. Models of mud-wave dynamics [*Flood*, 1988; *Blumsack and Weatherly*, 1989] predict that they are generally orientated

oblique to the prevailing flow direction. The causative flow for such waves can be either along-slope bottom currents or downslope turbidity currents [*Flood*, 1994; *Wynn et al.*, 2000]. Here, subsurface layering indicates upslope and down-current migration in a broadly southwesterly direction, although we acknowledge that obtaining a current direction from two-dimensional seismic lines is difficult [*Wynn and Stow*, 2002]. Upstream current velocity is lower on the upstream face and therefore deposition preferably takes place there, while less deposition and possible erosion occurs on the downstream flank where bottom flow accelerates [*Flood*, 1988]. This flow regime generates the slightly asymmetric character of the waves which indicates that processes maintaining these waves are currently active [*Manley and Flood*, 1993].

2.4.2. Trough-Filling Mechanisms

[29] It is obviously difficult to assess the relative importance of turbiditic and current-deposited sediment within the trough itself. To what extent are trough sediments carried in by bottom currents from elsewhere or are they simply resculpted? The narrow deep channel structure observed in Profile 6 provides an important indication (Figure 11). This filled channel runs north-south down the Falkland Plateau toward the trough and it was undoubtedly cut by turbidity currents. The base of the channel is at least at 2.95 s or >2.2 km below sea level. This depth is beneath the present-day trough fill as one might expect and also shows that the units fed by the channel are no younger than Unit II and most probably Unit I. In that case, Unit I predates drift formation since the channel must have filled rapidly as the drift grew. During the early history of the trough, the channel would have acted as a turbidity current conduit, taking material from the plateau to the deep-water trough. Today, the eastern end of the trough shallows to 3100 m from depths of up to 3740 m further west. One possibility, therefore, is that the current of Weddell Sea Deep Water (WSDW) transported sediments swept off the south side of the trough as described by *Cunningham and Barker* [1996]. Of course, onset of drift formation does not necessarily mean that axial supply of turbidite sediments ceased.

3. Chronostratigraphic Framework

3.1. Initial Hypothesis

[30] Previous studies have demonstrated the influence of ACC bottom flow on sedimentation on the slope and floor of the Falkland Trough [*Howe et al.*, 1997; *Cunningham et al.*, 1998, 2002]. DSDP cores also provide evidence that the Falkland Plateau itself has been subject to prolonged non-deposition or erosion since early Miocene times [*Barker et al.*, 1976]. Drift inception in this area is probably related to the onset of deep-water ACC flow as the Drake Passage gateway opened. Spreading in the Drake Passage could have started at 26.5 Ma but it would initially have led to only a shallow opening [*Barker and Burrell*, 1977]. Neither an entirely shallow (i.e., continental shelf) path nor an incomplete path would have led to the creation of a large ACC [*Barker*, 2001]. While opening of the Tasman Gateway began at about 35.5 Ma and was completed by 30.2 Ma [*Shipboard Scientific Party*, 2001], the dating of the opening of the Drake Passage is more difficult to determine because of the lack of suitable well data. *Barker* [2001] argues that it took place at 20–22 Ma, while *Lawver and Gahagan* [2003] have proposed a much earlier date (~31 Ma). *Livermore et al.* [2007] also suggest a pre-29 Ma inception. Contourite deposits within the Falkland Trough and Plateau together with drifts in the central Scotia Sea probably contain useful sedimentary constraints which would help to refine this date. Recent work by *Pfuhl and McCave* [2005] suggests an increase in flow speed and homogeneity of the Southern Ocean water masses near the Oligocene-Miocene boundary at 23.95 Ma (~23.0 Ma, according to *Lourens et al.* [2004]), which they relate to establishment of a complete ACC associated with the deep opening of Drake Passage. *Lyle et al.* [2007] have also used seismic and biostratigraphic evidence to support a post-25 Ma onset for the ACC. Assuming that the basal unconformity of the South Falkland Drift marks the onset of full ACC, the dating of this boundary would be an important contribution.

[31] In order to estimate ages of the four mapped sedimentary units of the SFSD and their bounding unconformities, we first determined average maximal unit thicknesses. Four representative profiles from the middle of the drift were chosen and the maximal thickness of each unit was estimated. Outlying profiles and cross-lines were excluded since their sedimentary cover has been thinned by erosion. We also avoided anomalous areas where large channel structures are observed. Calculated thicknesses are given in Table 2. It is difficult to determine sedimentation rates in the absence of local well data. However, Late Quaternary sedimentation rates can be obtained from a nearby

Table 2. Maximal Thicknesses and Standard Deviations of Individual Depositional Units Calculated for Seismic Reflection Profiles 1–4[a]

Contourite Layer	Maximal Thickness, m				Av. Max. Thickness, m
	Profile 1	Profile 2	Profile 3	Profile 4	
Unit 2B	55	52	62	60	57 ± 5
Unit 2A	62	61	70	58	63 ± 5
Unit 1B	254	208	138	190	198 ± 49
Unit 1A	176	196	239	168	195 ± 32

[a] Total maximal thickness is 625 m.

surface core, KC100, as well as from DSDP and ODP cores taken from Maurice Ewing Bank [*Howe et al.*, 1997] (Figure 1). Stratigraphic analysis of KC100, which is situated on the sloping Falkland Plateau in the eastern part of the trough, yields a sedimentation rate of 6 m/Ma for the interval 1.6–2.3 m. *Howe et al.* [1997] used diagnostic species to correlate this interval to the period 0.8–1.9 Ma. This core has highly condensed contourite sequences which indicate sustained periods of nondeposition and erosion related to intensified ACC activity during late Pliocene-early Pleistocene times [*Howe et al.*, 1997]. Sites 329 (DSDP Leg 36) and 512 (ODP Leg 71) are located close to Maurice Ewing Bank about 800 km from the Falkland Trough (Figure 1). Despite this great distance, we have exploited these cores because sedimentation took place under the influence of the deeper Lower Circumpolar Deep Water (LCDW) component of the ACC. Site 329, situated west of Maurice Ewing Bank in a water depth of 1520 m, was drilled to obtain the shallow-water Neogene biostratigraphic section [*Shipboard Scientific Party*, 1977]. This site provides sedimentation rates for the Miocene sequence, while Site 512 was targeted at the Oligocene-Miocene boundary [*Shipboard Scientific Party*, 1983]. This latter site is located east of the Maurice Ewing Bank in a water depth of 1845 m. The resultant sedimentation rates can be compared to values from the central Scotia Sea [*Maldonado et al.*, 2003] and from the Agulhas Ridge [*Schut et al.*, 2002] where contourite drifts related to ACC flow have also been observed. Sedimentation rates for these different locations are summarized in Table 3. They have considerable scatter. Lateral variations in the thicknesses of individual sediment units suggest that sediment rates are spatially variable as a consequence of changes in current intensity [*Faugères et al.*, 1993]. We have included all measured rates since it is hard to ascertain which values would be the most representative for the SFSD. Although KC100 is situated nearest to the drift, it is located beyond the data coverage in the area where the SFSD peters out. In contrast, values from the central Scotia Sea may be more appropriate to the Falkland Trough where rates can be expected to be high. An average sedimentation rate was then calculated for each sedimentary unit and the age of each unit was estimated (Table 4). Ages were also calculated using the maximal thickness of each unit, which minimizes the effect of erosional cut-out at sequence boundaries in the chronostratigraphic model. Our calculated ages suggest that the bulk of the SFSD formed during Miocene times. The base of the drift is dated at 20.6 Ma which corresponds to *Barker*'s [2001] estimate of ACC onset. Even allowing for the highest sedimentation rate, we do not obtain a date as old as 30 Ma.

3.2. Refinement

[32] The calculated dates of the internal sequence boundaries can be correlated to seismic stratigraphic sequences of other areas beneath the ACC such as the Agulhas Ridge and the central Scotia Ridge. The Agulhas Ridge lies along the Falkland-Agulhas Fracture Zone and was affected by the opening of gateways around Antarctica [*Lawver and Gahagan*, 2003; *Schut et al.*, 2002]. *Uenzelmann-Neben* [2001] identified three distinct reflections in mounded depositional sequences across the Agulhas Ridge which she has related to bottom-current activity. The dating of these reflections was determined from core data published by *Tucholke and Carpenter* [1977] and *Tucholke and Embley* [1984]. The other data set used for correlation is from the central Scotia Sea close to the Falkland Trough. *Maldonado et al.* [2003] defined six seismic stratigraphic units separated by unconformities which were deposited under the influence

Table 3. Estimated Sedimentation Rates and Associated Ages From Literature[a]

Age, Ma	Sedimentation Rate, m/Ma				
	KC100	Site 329	Site 512	Scotia Sea	Agulhas Ridge
Pleistocene	6	-	7	27	-
Pliocene	6	-	6	38	7.5
Late-middle Miocene	-	33.8	9.5	58	17
Middle-early Miocene	-	35.1	20	50–80	30

[a] See text for details.

Table 4. Sedimentation Rates and Standard Deviations Calculated From Published Values With Consequent Ages

Unit	Av. Sed. Rate, m/Ma	Est. Age, Ma		Adopted Age[a]	Sed. Rate, m/Ma	
		Max.	Av.		Max.	Av.
2B	13.3 ± 11.9	4.7	4.3	4.5[1]	13.8	12.7
2A	14.4 ± 15.7	9.5	8.7	9.0[2]	15.6	14.0
1B	29.6 ± 21.5	18.1	15.3	14.5[3]	46.2	35.9
1A	37.5 ± 19.4	24.5	20.5	23.0[4]	28.1	22.9

[a] These ages were adopted by assuming equivalence to significant climatic/circulation events, and both maximal and average sedimentation rates are inferred using this adopted age model. (1, *Coates et al.* [1992], *Farrell et al.* [1995], *Droxler et al.* [1998]; 2, *Zhou and Kyte* [1992], *Handwerger and Jarrard* [2003]; 3, *Hall et al.* [2003], *Handwerger and Jarrard* [2003]; 4, *Pfuhl and McCave* [2005], *Handwerger and Jarrard* [2003].)

of an eastward flowing ACC and a northward outflow of WSDW. Ages were estimated using the same method which we have used. *Uenzelmann-Neben* [2001] and *Maldonado et al.* [2003] suggest that the oldest unconformity (i.e., yellow surface) at the base of the drift formed at initiation of the ACC. *Uenzelmann-Neben* [2001] assumes an Early/Middle Oligocene age. However, *Maldonado et al.* [2003] determined the onset of the drift in the central Scotia Sea to be of early Miocene age, based on basement age, which is in accordance with our calculated age of the base of the SFSD.

[33] We estimate the second unit boundary within the SFSD (i.e., green horizon) to be of middle Miocene age (14.5 Ma, Table 4). *Uenzelmann-Neben* [2001] and *Maldonado et al.* [2003] attributed a reflection of this age to changes in the global bottom-current regime. At the Agulhas Ridge, it is related to erosion and redeposition associated with Antarctic bottom water [*Uenzelmann-Neben*, 2001]. In the central Scotia Sea, it is probably the result of openings in the South Scotia Ridge which allowed northern portions of WSDW to flow through the Jane Basin and gaps in the ridge [*Maldonado et al.*, 2003]. On the seismic profiles presented here, this event is often marked by a change from transparent to more reflective seismic facies. *Hall et al.* [2003] document a change in speed of the southwest Pacific deep western boundary current and a brief hiatus at this time, while *Handwerger and Jarrard* [2003] document a reduction in the sedimentation rate around Antarctica.

[34] The mid-Miocene increase in $\delta^{18}O$ from 15–10 Ma is usually associated with major Antarctic ice-sheet growth, which led to a period of significant global cooling at 14–14.5 Ma [*Shackleton and Kennett*, 1975; *Zachos et al.*, 2001]. However, it has also been described as deep-water cooling of 4–5°C leading to increases in ice volume and a drop in sea-level at 11–10 Ma [*Miller et al.*, 1987]. *Shevenell et al.* [2004] present a Mg/Ca-derived sea-surface temperature reconstruction for the South Tasman Rise across the mid-Miocene cooling event, which shows a stepwise drop over 300 ka preceding the increase in planktonic $\delta^{18}O$ lasting 100 ka and also, more importantly, a rather abrupt increase in benthic $\delta^{18}O$. They also show that the drop in temperature precedes a positive peak in foraminiferal $\delta^{13}C$ (a minimum in pCO_2), which implies that changes in the carbon cycle, often cited at other climate transitions, was not the key driving or amplifying force. *Shevenell et al.* [2004] prefer an explanation which requires strengthening of the ACC caused by further closure of the eastern Tethys [e.g., *Woodruff and Savin*, 1989; *Flower and Kennett*, 1993] as the likely trigger which drove climate across a threshold. We note that closure of the Indonesian Gateway to major throughflow at about 15 Ma could have served as another factor in causing mid-Miocene cooling [*Hall*, 2002].

[35] The third unit boundary (magenta horizon) within the SFSD is inferred to have formed during late Miocene times which corresponds again to a known event in the other two data sets. *Uenzelmann-Neben* [2001] suggests that this strong reflection formed due to erosion and redeposition of sediments by Circumpolar Deep Water within the ACC. At the Agulhas Ridge, the hiatus is often close to and thus indistinguable from the seafloor [*Uenzelmann-Neben*, 2001], an observation that is equivalently valid for the SFSD. In the central Scotia Sea, this event was related to a reorganization of bottom current flow that may predate the onset of grounded ice sheets on the Antarctic Peninsular shelf [*Maldonado et al.*, 2003]. Globally, this event is known from around Antarctica, dated by *Handwerger and Jarrard* [2003] at 9 Ma, and from the Pacific by *Zhou and Kyte* [1992], dated at 8.5 Ma. We have assigned an age of 9 Ma to this

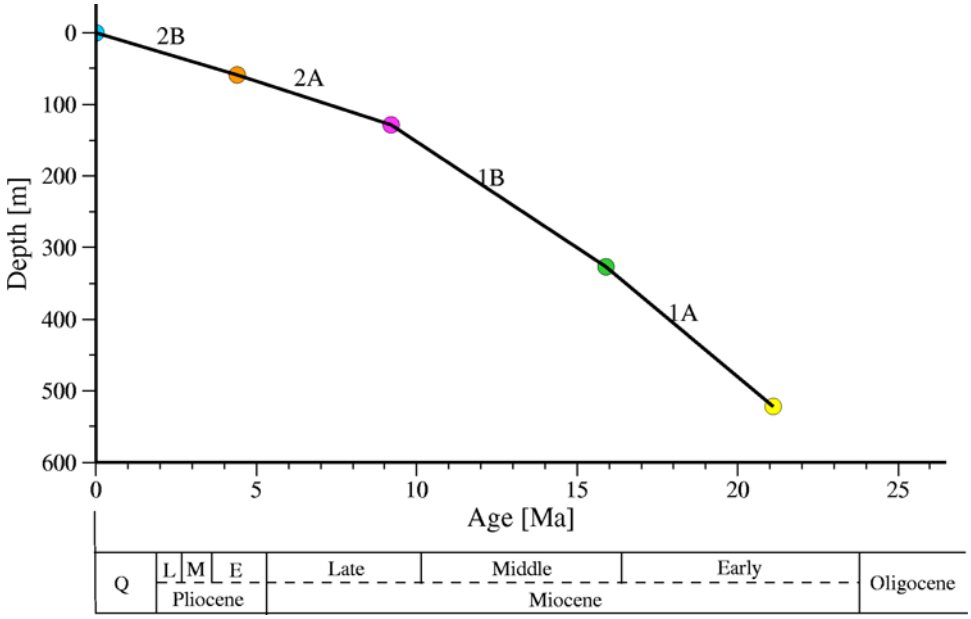

Figure 15. Maximal thickness of mapped units plotted as function of geologic age. This diagram was constructed by assuming that base of contourite deposit occurs at 21 Ma. To start with, sedimentation rate was assumed to be constant. Rates were then adjusted slightly to ensure that boundaries between mapped units correspond to geologically significant events which occur within realm of Antarctic Circumpolar Current.

reflection (Table 4 and Figure 15). Finally, an early Pliocene age is estimated for the youngest unconformity (orange horizon) which may be linked to opening of the Panama Seaway, to the onset of major Northern Hemisphere glaciation, or to the greater expansion of Antarctic ice sheets during late Pliocene times [*Maldonado et al.*, 2003]. Although this reflective surface is recognized in the Agulhas Ridge data, it was not dated there. We have assigned an age of 4.5 Ma to this event, based upon sedimentation rates.

3.3. Paleoceanographic Pathways

[36] The present-day flow path of the ACC is defined by reduced depositional thicknesses and the presence of moats and channels. Paired moats at the base of the trough clearly show the effects of a focussed filament of the present-day flow. Filled moats at earlier times are obviously a very useful guide for pinpointing the location of ancient flows. About 23 Ma ago, a flow began to transport substantial amounts of sediment from the west, favoring accumulation of the SFSD. Given that this drift is situated at depths of 500–1500 m, this area must previously have been occupied by some type of Southern Source Intermediate Water (SSIW). The basal unconformity therefore marks the change-over between this, presumably sluggish, SSIW flow and the ACC, which probably also carried SSIW. We suggest that sedimentation rates were high in early Miocene times, decreasing from 36–46 m/Ma to 13–15 m/Ma after 9 Ma in the late Miocene to Pleistocene period. Late Pleistocene rates are very low [*Howe et al.*, 1997]. The mid-Miocene maximum between 14.5 to 9 Ma is probably due to a combination of sediment supply and flow speed. A low early Pleistocene sedimentation rate exists despite the fact that fluctuations of sea level occur, which elsewhere have been responsible for pumping significant quantities of sediment off the shelf. We ascribe it to strong current suppression of accumulation.

[37] Along the base of the slope, topographic depressions were infilled as the pile of trough sediments grew, whereas drift deposition was concentrated on mid-slope regions. Orientations of the axes of contourite drifts reflect slope-controlled current flow. The increase in thickness and width of the SFSD toward the northeast suggests one possibility: the Falkland Islands became an important source of sediment for drift construction, especially for deposition of Unit 1B when sedimentation rates were highest. This sediment supply might also have triggered the shift in current axis (i.e., maximum thickness axis) for this unit. However, the shift could also be related to deepening of the gateway, allowing the ACC to flow between Tierra del Fuego and Burdwood Bank. Equally,

ACC flow strength could have decreased, or the altered density structure of the water column could have triggered a shift in the axis of maximum speed. It is probably reasonable to conclude that major deposition occurs upslope of the main axis of flow [e.g., *McCave and Tucholke*, 1986]. We also suggest that upslope migration of the locus of maximum deposition is controlled by an increase in ACC flow speed, especially after deposition of Unit 1A. Finally, the sharp pinch-out at 600 m water depth across the plateau surrounding the Falkland Islands is controlled by strong wind-driven currents on the shelf.

[38] The sediment waves observed on the southern slopes of the trough also reflect flow distribution patterns. Mud waves are developed by the interaction of persistent thermohaline bottom currents, fine grained sediment and preexisting topography [*Manley and Flood*, 1993]. In the southern hemisphere, mud waves tend to form at an angle which is counterclockwise to the prevailing current direction. These waves migrate up-current and to the left of the current [*Flood et al.*, 1993]. As the mud waves show a principal migration direction upslope and down-current toward the south (although the exact direction is not known), this observation is consistent with a slope-parallel flow from east to west giving a cyclonic (i.e., clockwise) circulation within the trough [*Blumsack*, 1993]. Although no studies have yet resolved the bottom current regime west of Burdwood Bank, *Cunningham et al.* [2003] suggest that ACC flow shallower than 400 m emerging from Drake Passage could pass over the sill between Burdwood Bank and South America. This flow trends northeast along the south Falkland Plateau slope. The mud waves observed here provide evidence of a westward flow along the trough.

4. Conclusions

[39] The reprocessed seismic data presented here can be used to document the detailed growth of a contourite deposit. Four sediment units are defined which indicate varying accumulation patterns and rates, which result from changes in oceanographic and climatic boundary conditions affecting the Southern Ocean. Unconformities separating the different seismic units have been correlated with major climatic and sedimentation events recognized in areas where sedimentation has also been influenced by the ACC and/or global deep-water circulation. The drift is deposited on an unconformity which is inferred to be associated with the deep opening of Drake Passage and the consequential onset of deep ACC flow. The age of this basal layer was estimated to be of early Miocene age (24.5 – 20.5 Ma) which is in accordance with the late dates for ACC establishment of 22–17 Ma proposed by *Barker* [2001], 23 Ma by *Pfuhl and McCave* [2005], and <25 Ma by *Lyle et al.* [2007]. A bright and continuous horizon in the middle of the drift has an estimated age of 14.5 Ma which corresponds to the long-postulated timing of probable ACC strengthening. Close to the top of the drift, a significant unconformity has an inferred age of 9 Ma, when bottom currents in the Scotia Sea were reorganized. The youngest mappable horizon has an estimated age of 4.5 Ma. We also show seismic images from the Falkland Trough itself where a stack of turbiditic sediments have been resculpted to some extent by bottom currents. Filled moats and mud waves are well resolved. This deposit is a westward continuation of the West Falkland Trough Drift which was probably deposited by Weddell Sea Deep Water.

[40] No wells have been drilled in the western Falkland Trough and our chronostratigraphic framework is informed speculation. The reprocessed seismic data presented here constitute a high-quality site survey for drilling a sedimentary deposit which will reveal important aspects of ACC history and a trough infill which records the vertical motions at a major plate boundary. The best drilling location is at 58.7°W, 53.2°S, where Profiles 1, 7 and 9 intersect on top of the thickest part of the South Falkland Slope Drift. All four sediment units and unconformities could be penetrated at this location. A second hole could be drilled further west at 60°W, 53.4°S, targeting trough sediments and the diagenetic front in order to correlate them with SFSD stratigraphy. If such a hole were drilled to more than 1 km depth, it would establish whether there was a switch from turbidite to contourite sedimentation and, if so, when.

Acknowledgments

[41] D.K. is grateful to Clare College and to the Department of Earth Sciences for financial support. Field tapes of the GFI-93 seismic reflection survey were generously provided by WesternGeco Ltd. The OMEGA processing package and the GEOFRAME interpretational package were generously provided by Schlumberger Inc. We thank A. Crosby, J. Jackson, R. Jones, D. Lyness, C. Trowell, and N. Woodcock for their help. We thank D. Stow, S. Berne, and L. Labeyrie for their careful reviews. Several figures were made using Generic Mapping Tools of *Wessel and Smith* [1998]. Cambridge Earth Sciences contribution 9070.

References

Barker, P. F. (2001), Scotia Sea regional tectonic evolution: Implications for mantle flow and palaeocirculation, *Earth Sci. Rev.*, *55*, 1–39.

Barker, P. F., and J. Burrell (1977), The opening of Drake Passage, *Mar. Geol.*, *25*, 15–34.

Barker, P. F., and E. Thomas (2004), Origin, signature and palaeoclimatic influence of the Antarctic Circumpolar Current, *Earth Sci. Rev.*, *66*, 143–162.

Barker, P. F., I. W. D. Dalziel, and Shipboard Scientific Party (1976), Evolution of the southwestern Atlantic Ocean basin: Results from Leg 36 of Deep Sea Drilling Project, *Initial Rep. Deep Sea Drill. Proj.*, *36*, 993–1014.

Blumsack, S. L. (1993), A model for the growth of mudwaves in the presence of time-varying currents, *Deep Sea Res., Part I*, *40*, 963–974.

Blumsack, S. L., and G. L. Weatherly (1989), Observations of the nearby flow and a model for the growth of mudwaves, *Deep Sea Res., Part A*, *36*, 1327–1339.

Bry, M., N. White, S. Singh, R. England, and C. Trowell (2004), Anatomy and formation of oblique continental collision: South Falkland basin, *Tectonics*, *23*, TC4011, doi:10.1029/2002TC001482.

Callahan, J. E. (1972), The structure of deep water in the Antarctic Ocean, *Deep Sea Res., Part I*, *19*, 563–575.

Carter, L., and I. N. McCave (1994), Development of sediment drifts approaching an active plate margin under the SW Pacific deep western boundary current, *Paleoceanography*, *9*, 1061–1085.

Carter, L., R. M. Carter, and I. N. McCave (2004), Evolution of the sedimentary system beneath the deep Pacific inflow off eastern New Zealand, *Mar. Geol.*, *205*, 9–27.

Coates, A. G., J. B. C. Jackson, L. S. Collins, T. M. Cronin, H. J. Dowsett, L. M. Bybell, P. Jung, and J. A. Obando (1992), Closure of the Isthmus of Panama: The near-shore marine record of Costa Rica and western Panama, *Geol. Soc. Am. Bull.*, *104*, 814–828.

Cunningham, A. P., and P. F. Barker (1996), Evidence for westward-flowing Weddell Sea Deep Water in the Falkland Trough, western South Atlantic, *Deep Sea Res., Part I*, *43*, 643–654.

Cunningham, A. P., P. F. Barker, and J. S. Tomlinson (1998), Tectonics and sedimentary environment of the North Scotia Ridge region revealed by side-scan sonar, *J. Geol. Soc. London*, *155*, 941–956.

Cunningham, A. P., J. A. Howe, and P. F. Barker (2002), Contourite sedimentation in the Falkland Trough, western South Atlantic Ocean, in *Deep-Water Contourite Systems: Modern Drifts and Ancient Series, Seismic and Sedimentary Characteristics*, edited by D. A. V. Stow et al., *Geol. Soc. London Mem.*, *22*, 337–352.

Cunningham, S. A., S. G. Alderson, B. A. King, and M. A. Brandon (2003), Transport and variability of the Antarctic Circumpolar Current in Drake Passage, *J. Geophys. Res.*, *108*(C5), 8084, doi:10.1029/2001JC001147.

Davies, R. J. (2005), Differential compaction and subsidence in sedimentary basins due to silica diagenesis: A case study, *Geol. Soc. Am. Bull.*, *117*, 1146–1155.

Droxler, A. W., K. Burke, A. D. Cunningham, A. C. Hine, E. Rosencrantz, D. Duncan, P. Hallock, and E. Robinson (1998), Caribbean constraints on circulation between Atlantic and Pacific Oceans over the past 40 million years, in *Tectonic Boundary Conditions for Climate Reconstructions*, edited by T. J. Crowley and K. C. Burke, pp. 160–191, Oxford Univ. Press, New York.

Farrell, J. W., I. Raffi, T. R. Janecek, D. W. Murray, M. Levitan, K. A. Dadey, K.-C. Emeis, M. Lyle, J.-A. Flores, and S. Hovan (1995), Late Neogene sedimentation patterns in the eastern equatorial Pacific Ocean, *Proc. Ocean Drill. Program Sci. Results*, *138*, 717–756, doi:10.2973/odp.proc.sr.138.143.

Faugères, J.-C., M. L. Mézerais, and D. A. Stow (1993), Contourite drift types and their distribution in the North and South Atlantic Ocean basins, *Sediment. Geol.*, *82*, 189–203.

Faugères, J. C., D. A. V. Stow, P. Imbert, A. R. Viana, and R. B. Wynn (1999), Seismic features diagnostic of contourite drifts, *Mar. Geol.*, *162*, 1–38.

Flood, R. D. (1988), A lee wave model for deep-sea mud-wave activity, *Deep Sea Res., Part II*, *35*, 973–983.

Flood, R. D. (1994), Abyssal bedforms as indicators of changing bottom current flow: Examples from the U.S. east coast continental rise, *Paleoceanography*, *9*, 1049–1060.

Flood, R. D., A. N. Shor, and P. L. Manley (1993), Morphology of abyssal mudwaves at Project MUDWAVES sites in the Argentine Basin, *Deep Sea Res., Part II*, *40*, 859–888.

Flower, B. P., and J. P. Kennett (1993), Relations between Monterey formation deposition and middle Miocene global cooling: Naples Beach Section, California, *Geology*, *21*, 877–880.

Gordon, A. L. (2001), Inter-ocean exchange, in *Ocean Circulation and Climate*, *Int. Geophys. Ser.*, edited by G. Siedler and J. Church, pp. 303–316, Academic, New York.

Grose, T. J., J. A. Johnson, and G. R. Bigg (1995), A comparison between the FRAM (Fine Resolution Antarctic Model) results and observations in Drake Passage, *Deep Sea Res., Part I*, *42*, 365–388.

Hall, I. R., I. N. McCave, R. Zahn, L. Carter, P. C. Knutz, and G. P. Weedon (2003), Paleocurrent reconstruction of the deep Pacific inflow during the middle Miocene: Reflections of East Antarctic Ice Sheet growth, *Paleoceanography*, *18*(2), 1040, doi:10.1029/2002PA000817.

Hall, R. (2002), Cenozoic geological and plate tectonic evolution of SE Asia and the SW Pacific: Computer-based reconstructions and animations, *J. Asian Earth Sci.*, *20*, 353–434.

Handwerger, D. A., and R. D. Jarrard (2003), Neogene changes in Southern Ocean sedimentation based on mass accumulation rates at four continental margins, *Paleoceanography*, *18*(4), 1081, doi:10.1029/2002PA000850.

Hollister, C. D., R. D. Flood, and I. N. McCave (1978), Plastering and decorating in the North Atlantic, *Oceanus*, *21*, 5–13.

Howe, J. A., and C. J. Pudsey (1999), Antarctic Circumpolar Deep Water: A Quaternary paleoflow record from the northern Scotia Sea, South Atlantic Ocean, *J. Sediment. Res.*, *69*, 847–861.

Howe, J. A., M. S. Stoker, and D. A. V. Stow (1994), Late Cenozoic sediment drift complex, northeast Rockall Trough, North Atlantic Ocean, *Paleoceanography*, *9*, 989–999.

Howe, J. A., C. J. Pudsey, and A. P. Cunningham (1997), Pliocene-Holocene contourite deposition under the Antarctic Circumpolar Current, western Falkland Trough, South Atlantic Ocean, *Mar. Geol.*, *138*, 27–50.

Lawver, L. A., and L. M. Gahagan (2003), Evolution of Cenozoic seaways in the circum-Antarctic region, *Palaeogeogr. Palaeoclimatol. Palaeoecol.*, *198*, 11–37.

Livermore, R., C.-D. Hillenbrand, M. Meredith, and G. Eagles (2007), Drake Passage and Cenozoic climate: An open and shut case?, *Geochem. Geophys. Geosyst.*, *8*, Q01005, doi:10.1029/2005GC001224.

Lourens, L. J., F. J. Hilgen, N. J. Shackleton, J. Laskar, and D. Wilson (2004), The Neogene Period, in *A Geological Time Scale 2004*, edited by F. M. Gradstein, J. G. Ogg, and A. G. Smith, pp. 409–440, Cambridge Univ Press, Cambridge.

Lyle, M., S. Gibbs, T. C. Moore, and D. K. Rea (2007), Late Oligocene initiation of the Antarctic Circumpolar Current: Evidence from the South Pacific, *Geology*, *35*, 691–694, doi:10.1130/G23806A.1.

Maldonado, A., A. Barnolas, F. Bohoyo, J. Galindo-Zaldivar, J. Hernandez-Molina, F. Lobo, J. Rodriguez-Fernandez, L. Somoza, and T. Vazquez (2003), Contourite deposits in the central Scotia Sea: The importance of the Antarctic Circumpolar Current and the Weddell Gyre flows, *Palaeogeogr. Palaeoclimatol. Palaeoecol.*, *198*, 187–221.

Manley, P. L., and R. D. Flood (1993), Paleoflow history determined from mudwave migration—Argentine Basin, *Deep Sea Res., Part II*, *40*, 1033–1055.

McCave, I. N. (2008), Sediment sorting during transport and deposition of contourites, in *Contourites*, *Dev. Sedimentol.*, vol. 57, edited by M. Rebesco and A. Camerlenghi, in press, Elsevier, Amsterdam.

McCave, I. N., and I. R. Hall (2006), Size sorting in marine muds: Processes, pitfalls, and prospects for paleoflow-speed proxies, *Geochem. Geophys. Geosyst.*, *7*, Q10N05, doi:10.1029/2006GC001284.

McCave, I. N., and B. E. Tucholke (1986), Deep current-controlled sedimentation in the western North Atlantic Ocean, in *The Geology of North America*, vol. M, *The Western North Atlantic Region*, edited by P. R. Vogt and B. E. Tucholke, pp. 451–468, Geol. Soc. of Am., Boulder, Colo.

Miller, K. G., R. G. Fairbanks, and G. S. Mountain (1987), Tertiary oxygen isotope synthesis, sea-level history, and continental margin erosion, *Paleoceanography*, *2*, 1–19.

Nowlin, W. D., and J. M. Klinck (1986), The physics of the Antarctic Circumpolar Current, *Rev. Geophys.*, *24*, 469–491.

Orsi, A. H., T. Whitworth, III, and W. D. Nowlin, Jr. (1995), On the meridional extent and fronts of the Antarctic Circumpolar Current, *Deep Sea Res., Part I*, *42*, 641–673.

Pfuhl, H. A., and I. N. McCave (2005), Evidence for Late Oligocene establishment of the Antarctic Circumpolar Current, *Earth Planet. Sci. Lett.*, *235*, 715–728.

Rack, F. R. (1993), A geologic perspective on the Miocene evolution of the Antarctic Circumpolar Current system, *Tectonophysics*, *222*, 397–415.

Rintoul, S. R., C. W. Hughes, and D. Olbers (2001), The Antarctic Circumpolar Current System, in *Ocean Circulation and Climate*, edited by G. Siedler and J. Church, pp. 271–302, Academic, New York.

Schmitz, W. J.Jr. (1995), On the interbasin-scale thermohaline circulation, *Rev. Geophys.*, *33*, 151–173.

Schut, E. W., G. Uenzelmann-Neben, and R. Gersonde (2002), Seismic evidence for bottom current activity at the Agulhas Ridge, *Global Planet. Change*, *34*, 185–198.

Shackleton, N. J., and J. P. Kennett (1975), Paleotemperature history of the Cenozoic and the initiation of Antarctic glaciation: Oxygen and carbon isotopic analyses in DSDP Sites 277, 279, and 281, *Initial Rep. Deep Sea Drill. Proj.*, *29*, 743–755.

Shevenell, A. E., J. P. Kennett, and D. W. Lea (2004), Middle Miocene Southern Ocean cooling and Antarctic cryosphere expansion, *Science*, *305*, 1766–1770, doi:10.1126/science.1100061.

Shipboard Scientific Party (1977), Site 329, *Initial Rep. Deep Sea Drill. Proj.*, *36*, 143–206, doi:10.2973/dsdp.proc.36.105.1977.

Shipboard Scientific Party (1983), Site 512, *Initial Rep. Deep Sea Drill. Proj.*, *71*, 111–144, doi:10.2973/dsdp.proc.71.10.1983.

Shipboard Scientific Party (2001), Leg 189 summary, *Proc. Ocean Drill. Program Initial Rep.*, *189*, 98 pp., doi:10.2973/odp.proc.ir.189.101.2001.

Stow, D. A. V., J.-C. Faugères, A. Viana, and E. Gonthier (1998), Fossil contourites: A critical review, *Sed. Geol.*, *115*, 3–31.

Stow, D. A. V., , C. J. Pudsey, J. A. Howe, J. C. Faugères, and A. R. Viana (Eds.) (2002), *Deep-Water Contourite Systems: Modern Drifts and Ancient Series, Seismic and Sedimentary Characteristics*, *Geol. Soc. London Mem.*, vol. 22, pp. 337–352, Geol. Soc. of London, London.

Tucholke, B. E., and G. B. Carpenter (1977), Sediment distribution and Cenozoic sedimentation patterns on the Agulhas Plateau, *Geol. Soc. Am. Bull.*, *88*, 1337–1346.

Tucholke, B. E., and R. W. Embley (1984), Cenozoic regional erosion of the abyssal sea floor off South Africa, in *Interregional Unconformities and Hydrocarbon Accumulations*, edited by J. S. Schlee, *AAPG Mem.*, *36*, 145–164.

Uenzelmann-Neben, G. (2001), Seismic characteristics of sediment drifts: An example from the Agulhas Plateau, Southwest Indian Ocean, *Mar. Geophys. Res.*, *22*, 323–343.

Wessel, P., and W. H. F. Smith (1998), New improved version of Generic Mapping Tools released, *Eos Trans. AGU*, *79*, 579.

White, W., and R. Peterson (1996), An Antarctic circumpolar wave in surface pressure, wind, temperature and sea ice extent, *Nature*, *380*, 699–702.

Woodruff, F., and S. M. Savin (1989), Miocene deepwater oceanography, *Paleoceanography*, *4*, 87–140.

Wynn, R. B., and D. A. V. Stow (2002), Classification and characterisation of deep-water sediment waves, *Mar. Geol.*, *192*, 7–22.

Wynn, R. B., P. P. E. Weaver, G. Ercilla, D. A. V. Stow, and D. G. Masson (2000), Sedimentary processes in the Selvage sediment-wave field, NE Atlantic: New insights into the formation of sediment waves by turbidity currents, *Sedimentology*, *47*, 1181–1197.

Zachos, J., M. Pagani, L. Sloan, E. Thomas, and K. Billups (2001), Trends, rhythms, and aberrations in global climate 65 Ma to present, *Science*, *292*, 686–693, doi:10.1126/science.1059412.

Zhou, L., and F. T. Kyte (1992), Sedimentation history of the South Pacific red clay province over the last 55 million years inferred from the geochemistry of Deep Sea Drilling Project Hole 596, *Paleoceanography*, *7*, 441–465.